NASA Technical Paper 1351

Effects of Wing Leading-Edge Flap Deflections on Subsonic Longitudinal Aerodynamic Characteristics of a Wing-Fuselage Configuration With a 44° Swept Wing

William P. Henderson

NOVEMBER 1978

NASA

NASA Technical Paper 1351

Effects of Wing Leading-Edge Flap Deflections on Subsonic Longitudinal Aerodynamic Characteristics of a Wing-Fuselage Configuration With a 44° Swept Wing

William P. Henderson
Langley Research Center
Hampton, Virginia

SUMMARY

An investigation has been conducted to determine the effects of wing leading-edge flap deflections on the subsonic longitudinal aerodynamic characteristics of a wing-fuselage configuration with a 44° swept wing. The tests were conducted at Mach numbers from 0.40 to 0.85, corresponding to Reynolds numbers (based on wing mean geometric chord) of 2.37×10^6 to 4.59×10^6 and at angles of attack from -3° to 22°. The configurations under study included a wing-fuselage configuration and a wing-fuselage-strake configuration. Each configuration had multisegmented, constant-chord leading-edge flaps which could be deflected independently or in various combinations.

The results of this study indicate that the longitudinal aerodynamic drag characteristics for the configuration with the wing leading-edge flaps undeflected were only slightly affected by increasing Mach number. For the configuration with all the leading-edge flaps deflected down 16°, flow separation resulted in significant increases in drag with increasing Mach number. The combination of leading-edge flap deflections required to achieve minimum drag at the higher lift coefficients differs at the various Mach numbers tested, with a nose-down deflection of -16° achieving the lowest drag at a Mach number of 0.40. The theory utilized did not provide an adequate calculation of the absolute drag levels for the configurations studied. Deflecting simple leading-edge flaps provided a significant portion of the theoretically achievable drag reduction on the wing-fuselage configuration. For the wing-fuselage-strake configuration only a small portion of the theoretically achievable drag reduction was obtained. The theory provided a reasonable estimate of the drag increment due to flap deflections for the wing-fuselage configuration. For the wing-fuselage-strake configuration, however, the theory overpredicts the increment in drag.

INTRODUCTION

The maneuvering capability of aircraft engaged in air-to-air combat is often limited by flow separation over the wings. This flow separation can manifest itself in a variety of adverse factors such as buffeting, increased drag, and losses in lift and stability. The National Aeronautics and Space Administration is conducting studies to provide information for use in developing aircraft concepts which avoid these adverse factors. A summary of some of the research in this area is presented in reference 1. One investigation, the purpose of which was to improve the drag characteristics of a fighter aircraft at maneuvering conditions, is the subject of the present paper. Wing leading-edge flaps have been used to reduce the drag on fighter aircraft for some time. In most cases, however, the wing leading-edge flaps, because of weight considerations, are in one segment. Achieving an optimum wing shape at high angles of attack may require an increasing spanwise wing twist. (See ref. 2.) It would be very difficult to achieve this increasing wing twist on a wing having a single-segmented leading-edge flap. One method that could be utilized to vary

the wing-twist angle would be to use a multisegmented leading-edge flap. It is the purpose of this paper to compare the longitudinal aerodynamic characteristics of a wing-fuselage configuration and a wing-fuselage-strake configuration utilizing a single-segment leading-edge flap with the same wing-fuselage configuration utilizing a multisegmented leading-edge flap. Analytical calculation of flap effectiveness will also be presented as an aid in interpreting the data.

The study was conducted in the Langley high-speed 7- by 10-foot tunnel at Mach numbers from 0.40 to 0.85 and angles of attack from -3° to 22°.

SYMBOLS

The results presented in this paper are referred to the stability-axis system with the exception of the lift and drag coefficients, which are referred to the wind-axis system. The force and moment data are nondimensionalized with respect to the geometric characteristics of the wing planform with its leading and trailing edges extended into the fuselage center line. The moment reference center was located at a point 65.91 cm rearward of the nose along the model reference line. (See fig. 1.)

b wing span, 50.80 cm

C_D drag coefficient, $\dfrac{\text{Drag}}{qS}$

ΔC_D increment in drag between wing with flaps deflected and flaps undeflected

C_L lift coefficient, $\dfrac{\text{Lift}}{qS}$

C_m pitching-moment coefficient, $\dfrac{\text{Pitching moment}}{qS\bar{c}}$

c_t section leading-edge thrust coefficient, $\dfrac{\text{Section leading-edge thrust}}{qc}$

c wing local chord, cm

$\bar{c}$ wing mean geometric chord, 23.30 cm

M free-stream Mach number

q free-stream dynamic pressure, Pa

S wing reference area, leading and trailing edges extended into fuselage center line, 0.1032 m^2

2

y   distance from fuselage reference line (measured spanwise), cm

α angle of attack, deg

δ_f wing leading-edge flap deflection (positive leading edge up) used
with subscripts 1 to 5 to denote segment deflected, deg

MODEL DESCRIPTION

A three-view drawing of the basic model is presented in figure 1(a) and
a drawing showing the model with the wing strake is presented in figure 1(b).
A photograph of the sting-mounted model in the Langley high-speed 7- by 10-foot
tunnel is presented in figures 2 and 3. The model as illustrated in figure 1(a)
consists of a simple wing-fuselage configuration. The wing has an aspect ratio
of 2.5, a taper ratio of 0.20, a wing leading-edge sweep angle of 44°, and NACA
64A-series airfoil sections (measured streamwise) with a thickness ratio of
6 percent at the fuselage juncture which varies linearly to 4 percent at the
wing tip. The wing strake (fig. 1(b)) was constructed of a 0.159-cm-thick flat
plate with sharp leading edges. The sharp leading edge had a total bevel angle
of 3.2° and was sealed on the edge between the strake and the wing.

Both models had a constant-chord leading-edge flap which was segmented into
five flap segments. These segments could be deflected to the same angle, simu-
lating a one piece leading-edge flap, or to differing angles, simulating changes
in wing twist along the wing span. For the wing with the leading-edge strake
(fig. 1(b)), flap segment number 1 was located behind the strake and therefore
was not deflected. Flap segment number 2 was located partially behind the strake
(about 18 percent of its area); however, the entire flap segment was deflected
for this test.

TEST AND CORRECTIONS

The investigation was conducted in the Langley high-speed 7- by 10-foot
tunnel at Mach numbers from 0.40 to 0.85 and at angles at attack from -3° to 22°.
The variation of the test Reynolds number, based on the wing mean geometric
chord, is presented in the following table:

M	Reynolds number
0.40	2.37×10^6
.70	3.81
.75	4.10
.80	4.33
.85	4.59

Transition strips (0.32 cm wide) of No. 100 carborundum grains (based on anal-
ysis of ref. 3) were placed 1.14 cm streamwise behind the leading edge of the
wings and 2.54 cm behind the nose of the fuselage.

Corrections to the model angle of attack have been made for deflections of the balance and sting support system due to aerodynamic load. Pressure measurements obtained from orifices located within the fuselage base cavity were used to adjust the drag coefficient to a condition of free-stream static pressure at the model base. Jet-boundary and blockage corrections estimated by the procedures of references 4 and 5, respectively, were applied to the data.

PRESENTATION OF RESULTS

The results obtained in this investigation are given in the figures as follows:

RESULTS AND DISCUSSION

The longitudinal aerodynamic characteristics for the configuration with the leading-edge flaps undeflected are presented in figure 4. The drag characteristics are only slightly affected by increasing Mach number. There is an indication of flow separation occurring on the wing, as evidenced by the break in lift-curve slope at an angle of attack of about 8°. This flow separation appears to occur on the forward portion of the wing (ahead of the moment reference point) since the separation results in a reduction in pitching-moment coefficient. With the wing leading-edge flaps deflected -16°, flow separation results in a significant increase in drag (see fig. 5) as Mach number is increased. This can be expected since deflecting leading-edge flaps on thin wings usually results in a fairly pronounced discontinuity at the flap hinge line.

The effects of various combinations of wing leading-edge flap deflections on the longitudinal aerodynamic characteristics of the wing-fuselage configuration (strake off) at M = 0.40 and 0.80 are presented in figures 6 and 7, respectively. It is interesting to note that the flap deflections required to achieve the minimum drag at a lift coefficient of 0.80 differ at the two Mach numbers studied. At the lower Mach number all leading-edge flaps deflected -16° resulted in the lowest drag; however, at a Mach number of 0.80 the lowest drag occurred for deflection angles varying along the wing span from -8° to -20°. It would appear that separation effects may be more significant on the inboard portion of the wing at the higher Mach numbers.

The increment in drag associated with deflection of the wing leading-edge flaps is small for the wing-fuselage-strake configuration as shown in figures 8 and 9. The dashed curve in figure 8 represents aerodynamic data for the wing-fuselage-strake configuration with all flaps undeflected. The data were not obtained from tests conducted during this study, but were obtained from as yet unpublished data obtained by Edward J. Ray of Langley Research Center. The only data available were obtained at a Mach number of 0.40, and no similar data were available for a Mach number of 0.80. It was anticipated that, for the wing-fuselage-strake configuration (based on unpublished wing-design studies), higher inboard deflection angles would be required to give the minimum drag coefficient for a specific lift coefficient. This is the opposite of that normally required on swept wings, where increasing outboard deflections yield the lowest drag coefficient. The data of figures 8 and 9 indicate that the increment in drag associated with flap deflections was considerably less for the wing with the strake than for the wing without the strake. (See figs. 6 and 7.) The data also indicated that the wing with the flaps deflected -16° resulted in the lowest drag at the higher lift coefficients at M = 0.40, and that the

wing with the flaps deflected from -8° inboard to -20° outboard resulted in the lowest drag at M = 0.80. It is not readily understood why these results occur; however, some insight may be gained with the aid of figures 10 to 15.

Figures 10 to 12 present the drag for each configuration with the leading-edge flaps deflected 0°, -8°, and -16° compared with estimates for full and zero leading-edge suction. A definition of full and zero suction is presented in reference 6. The data for the wing-fuselage configuration with the flaps undeflected departs from the full-suction curve (fig. 10 or 11) at low lift coefficients, which indicates a loss of leading-edge suction through flow separation. At the higher lift coefficients, the flow separation is much more extensive, as evidenced by the experimental drag being higher than the zero suction drag. As the leading-edge flaps are deflected, the experimental drag levels are reduced and agree with the full-suction curve in the intermediate lift-coefficient range. It is interesting to note that the drag levels at lift coefficients up to 0.60 (fig. 10) for the wing with flaps deflected -16° is equivalent to the full-suction drag even though the camber surface with flaps deflected is not an optimum camber shape for minimum drag. If the wing with the flaps deflected -16° represented an optimum camber shape, then the zero-suction curve would be tangent to the full-suction curve at the optimum lift coefficient. The trends in the data indicate that part of the drag reduction is due to suction pressure distributed over the wing camber surface and part is due to suction developed at the wing leading edge.

A calculation combining zero and full leading-edge suction on the wing with vortex flow on the strake is presented in figure 12 in addition to the potential-flow estimates previously discussed. Vortex lift on the strake reduces the zero leading-edge suction drag and increases the full-suction level. The experimental data at all three wing leading-edge flap-deflection angles presented in this figure remains very close to the zero-suction levels indicating that vortex flows may affect the formation of leading-edge suction on the wings.

A comparison between the calculated and experimentally determined increment in drag due to leading-edge flap deflection is presented in figures 13 to 15. As previously shown by the data of figures 10 to 12, the calculation procedures used are not adequate for predicting the absolute drag levels. However, as indicated in figures 13 and 14, the analytical procedures predict the increment in drag due to leading-edge flap deflection for the wing-fuselage configuration with a reasonable degree of accuracy at the low-to-intermediate lift coefficients. At the higher lift coefficients, the theory underpredicts the increment in drag primarily because the reference wing (flaps undeflected) exhibits flow separation on the wing which is not present on the wing with flaps deflected. For the wing-fuselage-strake configuration (fig. 15) the theory overpredicts the increment in drag due to wing leading-edge flap deflection, which indicates again that vortex flows appear to limit the formation of the apparent wing leading-edge thrust.

In the discussions associated with figure 6 it was pointed out that the minimum drag at lift coefficients of about 0.80 was obtained when the five flap

6

segments were deflected −16°. Variations of the optimum leading-edge flap
deflection angle with wing span are presented in figure 16. The variations
were calculated, using the theory of references 7 and 8, by James L. Thomas of
Langley Research Center. It can be seen that the leading-edge thrust variation
is relatively flat along the wing span except in the region of the wing tip,
the wing-fuselage juncture, and the wing-strake juncture. This type of suction
distribution results in a fairly constant variation of flap-deflection angle
along the wing leading edge, and only about a 3.5° variation for an angle of
attack of 10°. (See bottom section of fig. 16.) Although the optimum varia-
tion of leading-edge flap deflection was not investigated experimentally, the
incremental drag associated with the optimum variation was calculated and is
presented in figures 17 and 18. In these figures this calculation is compared
with the experimental data and a calculation for the wing with −16° of leading-
edge flap deflection along the wing span. Since the −16° flap variation is
fairly close to the optimum deflection angles, the calculated drag increments
are nearly the same. In addition, it is obvious from these data (fig. 17) that
for the wing-fuselage configuration (no strake) the theory provides a reasonable
estimate of the drag due to flap deflections and that simple wing leading-edge
flap deflections provide a significant portion of the theoretically achieved
drag reduction. For the wing-fuselage-strake configuration (fig. 18), the con-
stant variation of leading-edge flap deflections appears to be near the optimum.
Again it should be noted that the theory overpredicts the incremental drag vari-
ations such that leading-edge flaps provide only a small portion of the theoret-
ically achieved drag reduction.

CONCLUSIONS

     A study has been conducted to determine the effects of wing leading-edge
flap deflections on the subsonic longitudinal aerodynamic characteristics of a
wing-fuselage configuration with a 44° swept wing. As a result of this study,
the following conclusions can be made:

     1. The drag characteristics for the configuration with the wing leading-
edge flaps undeflected were only slightly affected by increasing Mach number.
For the configuration with the flaps deflected −16°, flow separation resulted
in a significant increase in drag with increasing Mach number.

     2. The combination of flap deflection required to achieve minimum drag at
the higher lift coefficients differed at the various Mach numbers tested. A
constant −16° deflection achieved the lowest drag at a Mach number of 0.40.

     3. The theory utilized did not provide an adequate calculation of the
absolute drag levels for the configuration studied.

     4. Deflecting simple leading-edge flaps provided a significant portion of
the theoretically achieved drag reduction on the wing-fuselage configuration.
For the wing-fuselage-strake configuration only a small portion of the theoret-
ically achieved drag reduction was obtained.

5. The theory provided a reasonable estimate of the drag increment due to flap deflection for the wing-fuselage configuration. For the wing-fuselage-strake configuration, however, the theory overpredicts the increment in drag.

Langley Research Center
National Aeronautics and Space Administration
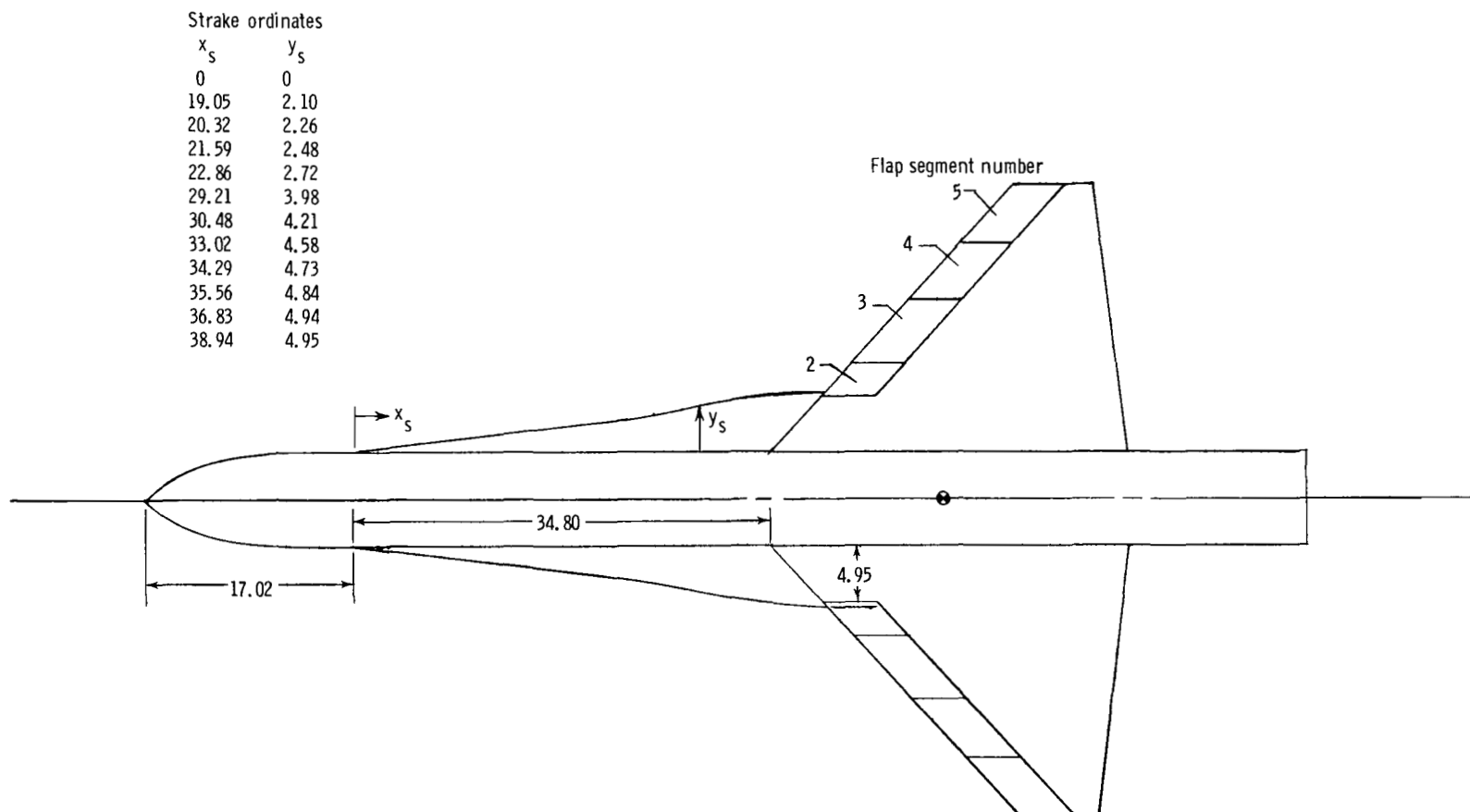Hampton, VA 23665
October 5, 1978

REFERENCES

1. Ray, Edward J.; McKinney, Linwood W.; and Carmichael, Julian G.: Maneuver and Buffet Characteristics of Fighter Aircraft. NASA TN D-7131, 1973.

2. Henderson, William P.; and Huffman, Jarrett K.: Effect of Wing Design on the Longitudinal Aerodynamic Characteristics of a Wing-Body Model at Subsonic Speeds. NASA TN D-7099, 1972.

3. Braslow, Albert L.; Hicks, Raymond M.; and Harris, Roy V., Jr.: Use of Grit-Type Boundary-Layer-Transition Trips on Wind-Tunnel Models. NASA TN D-3579, 1966.

4. Gillis, Clarence L.; Polhamus, Edward C.; and Gray, Joseph L., Jr.: Charts for Determining Jet-Boundary Corrections for Complete Models in 7- by 10-Foot Closed Rectangular Wind Tunnels. NACA WR L-123, 1945. (Formerly NACA ARR L5G31.)

5. Herriot, John G.: Blockage Corrections for Three-Dimensional-Flow Closed-Throat Wind Tunnels, With Consideration of the Effect of Compressibility. NACA Rep. 995, 1950. (Supersedes NACA RM A7B28.)

6. Henderson, William P.: Studies of Various Factors Affecting Drag Due to Lift at Subsonic Speeds. NASA TN D-3584, 1966.

7. Lamar, John E.: A Modified Multhopp Approach for Predicting Lifting Pressures and Camber Shape for Composite Planforms in Subsonic Flow. NASA TN D-4427, 1968.

8. Lamar, John E.: Some Recent Applications of the Suction Analogy to Vortex-Lift Estimates. Aerodynamic Analyses Requiring Advanced Computers, Part II, NASA SP-347, 1975, pp. 985-1011.

8
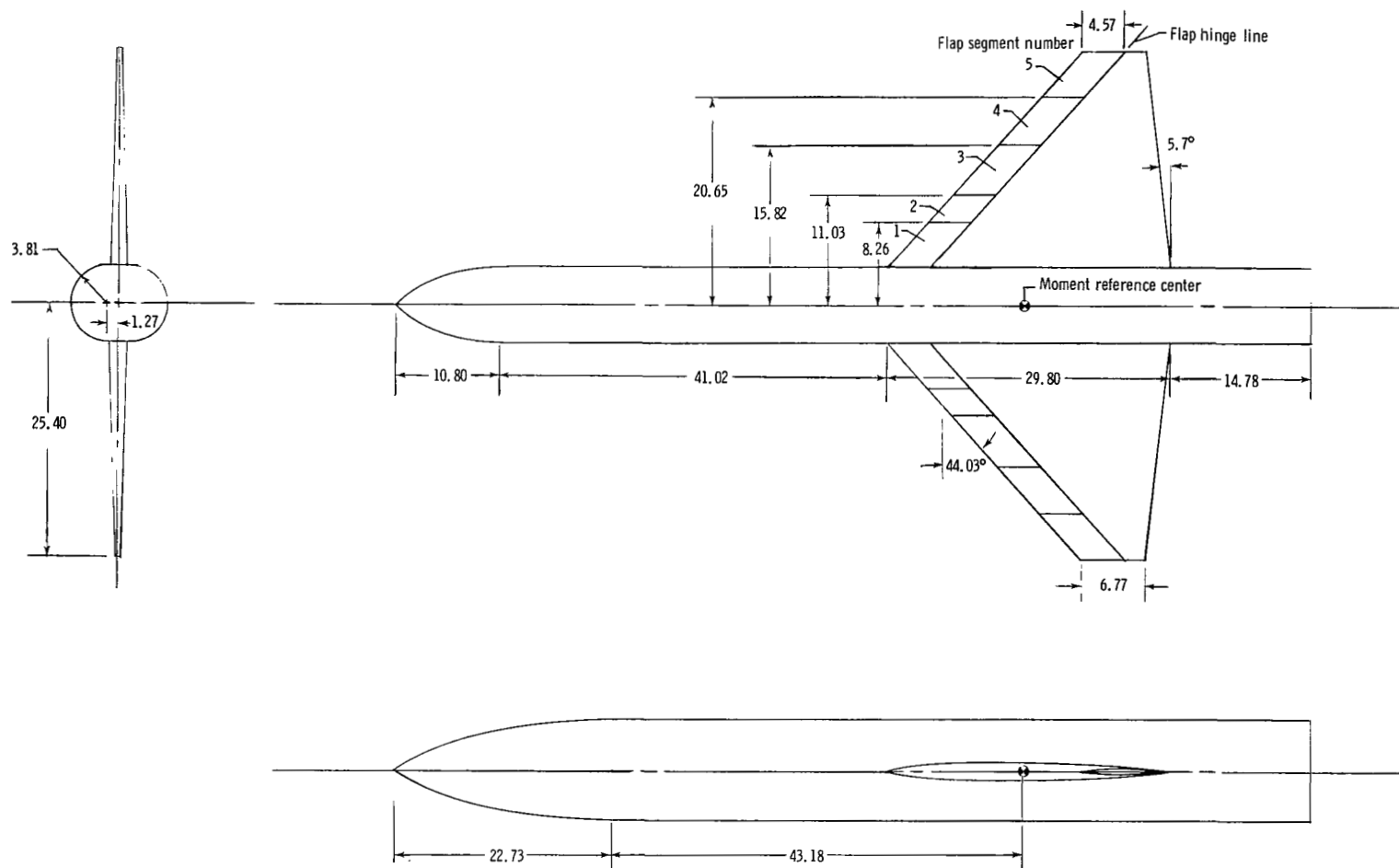
(a) Wing-fuselage model.

Figure 1.- Drawing of configurations under study. Dimensions are in centimeters unless
otherwise noted.

Strake ordinates

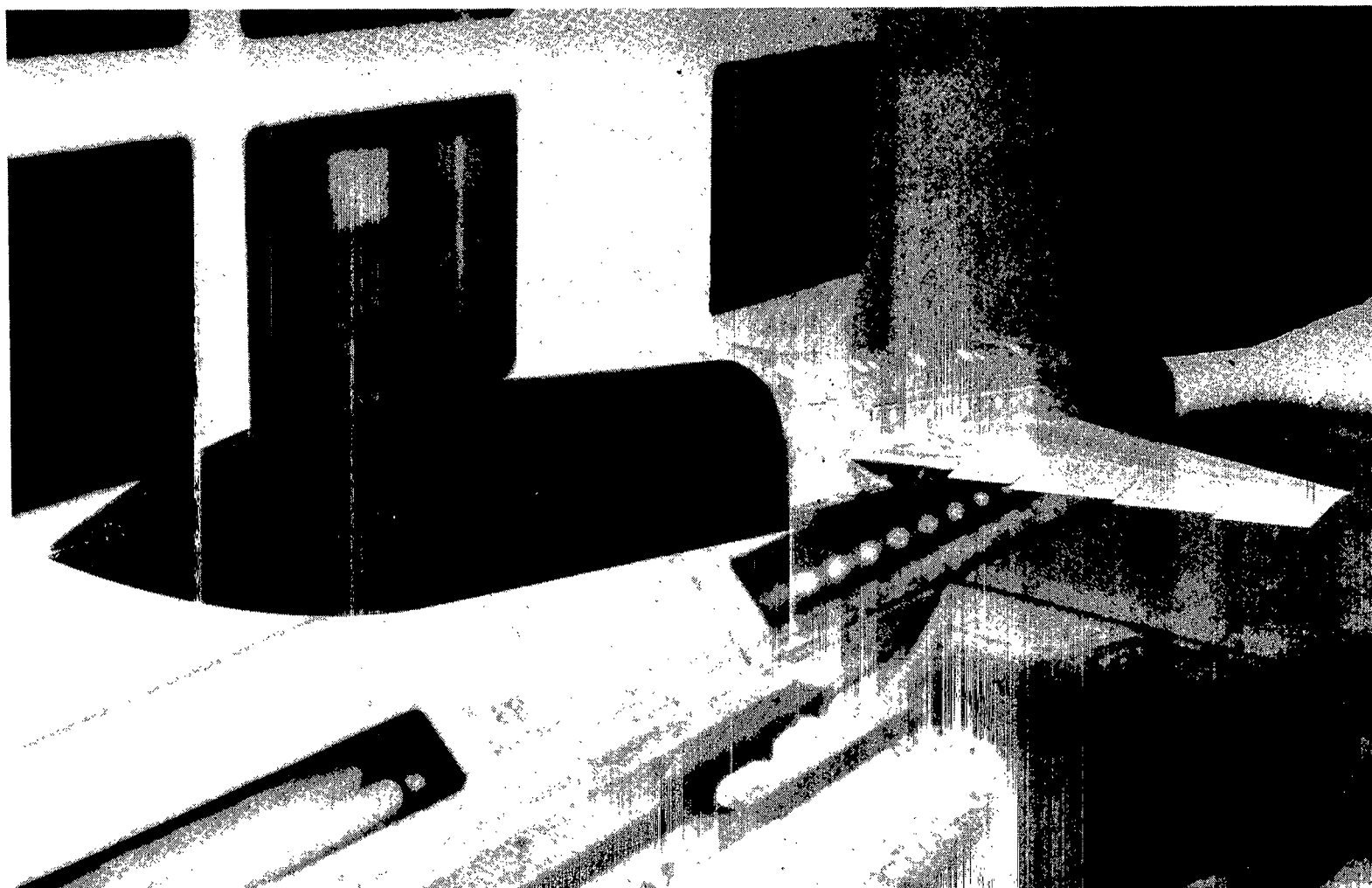| x_s	y_s
0	0
19.05	2.10
20.32	2.26
21.59	2.48
22.86	2.72
29.21	3.98
30.48	4.21
33.02	4.58
34.29	4.73
35.56	4.84
36.83	4.94
38.94	4.95

Flap segment number

5

4

3

2

x_s

y_s

34.80

17.02

4.95

(b) Wing-strake model.

Figure 1.- Concluded.
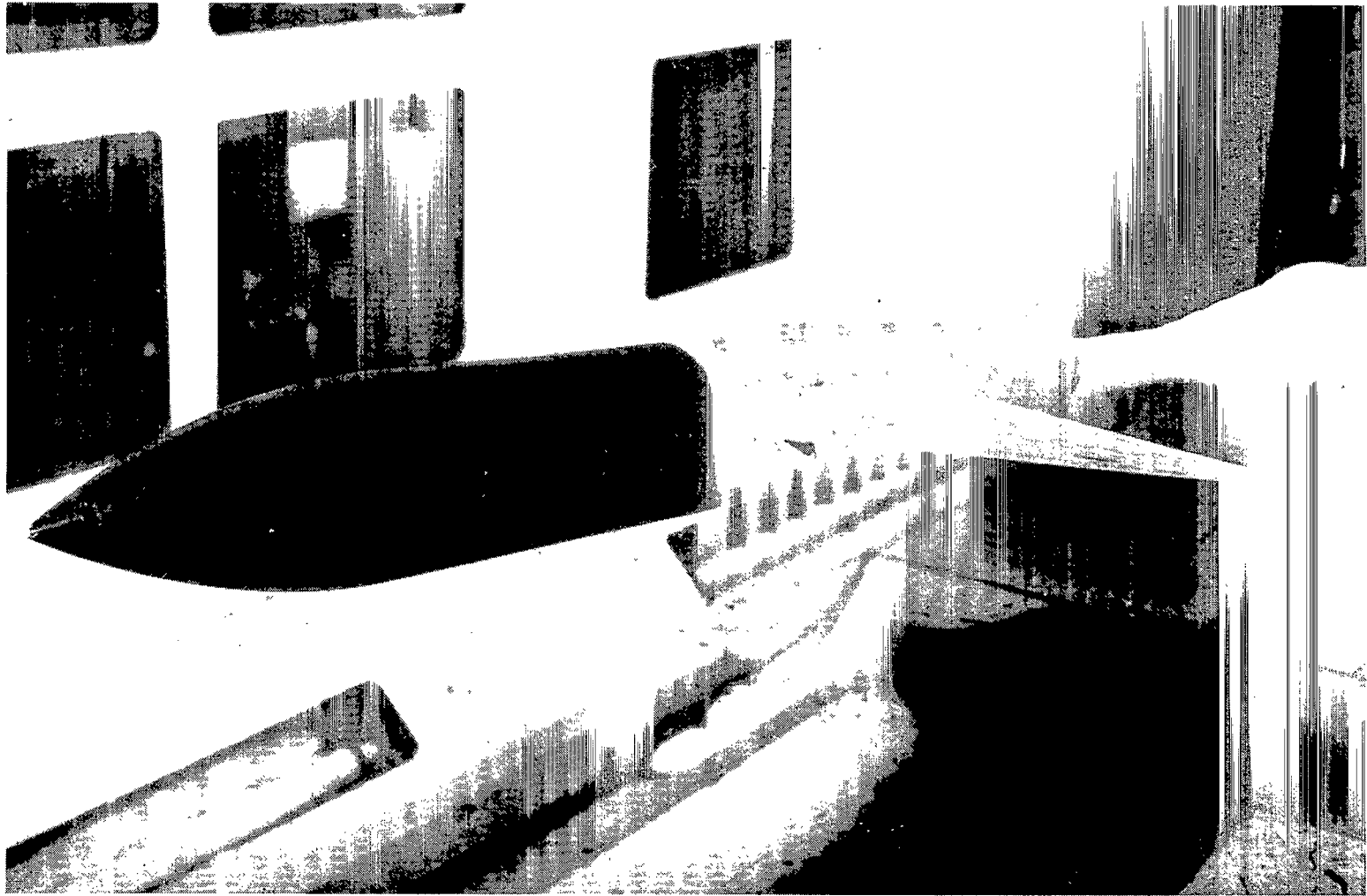
L-76-7233

(a) Flaps undeflected.

Figure 2.- Wing-fuselage model in Langley high-speed 7- by 10-foot tunnel.

L-76-7235

(b) Flaps deflected.

Figure 2.- Concluded.
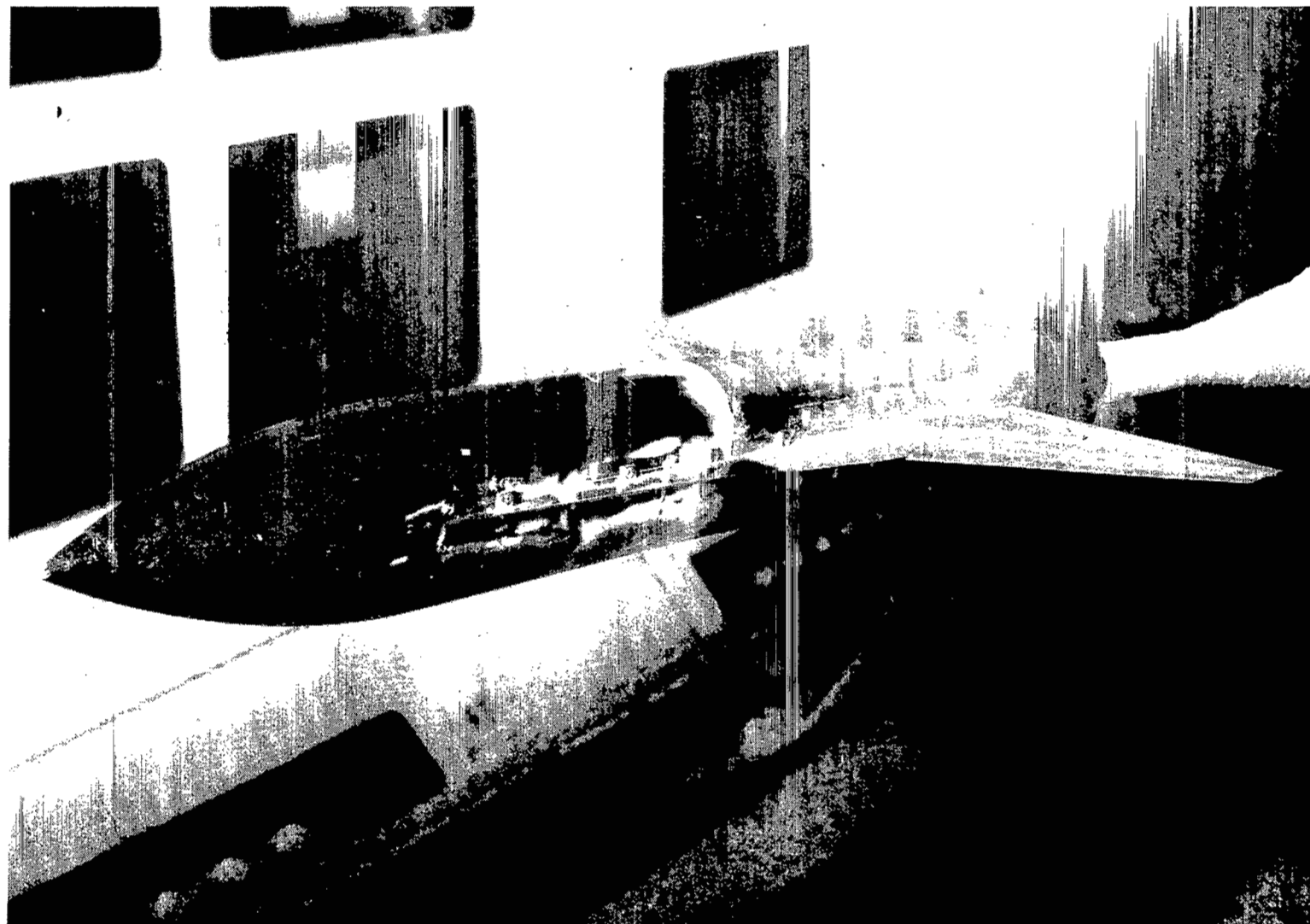
L-76-7236

(a) Flaps undeflected.

Figure 3.- Wing-fuselage-strake model in Langley high-speed 7- by 10-foot tunnel.
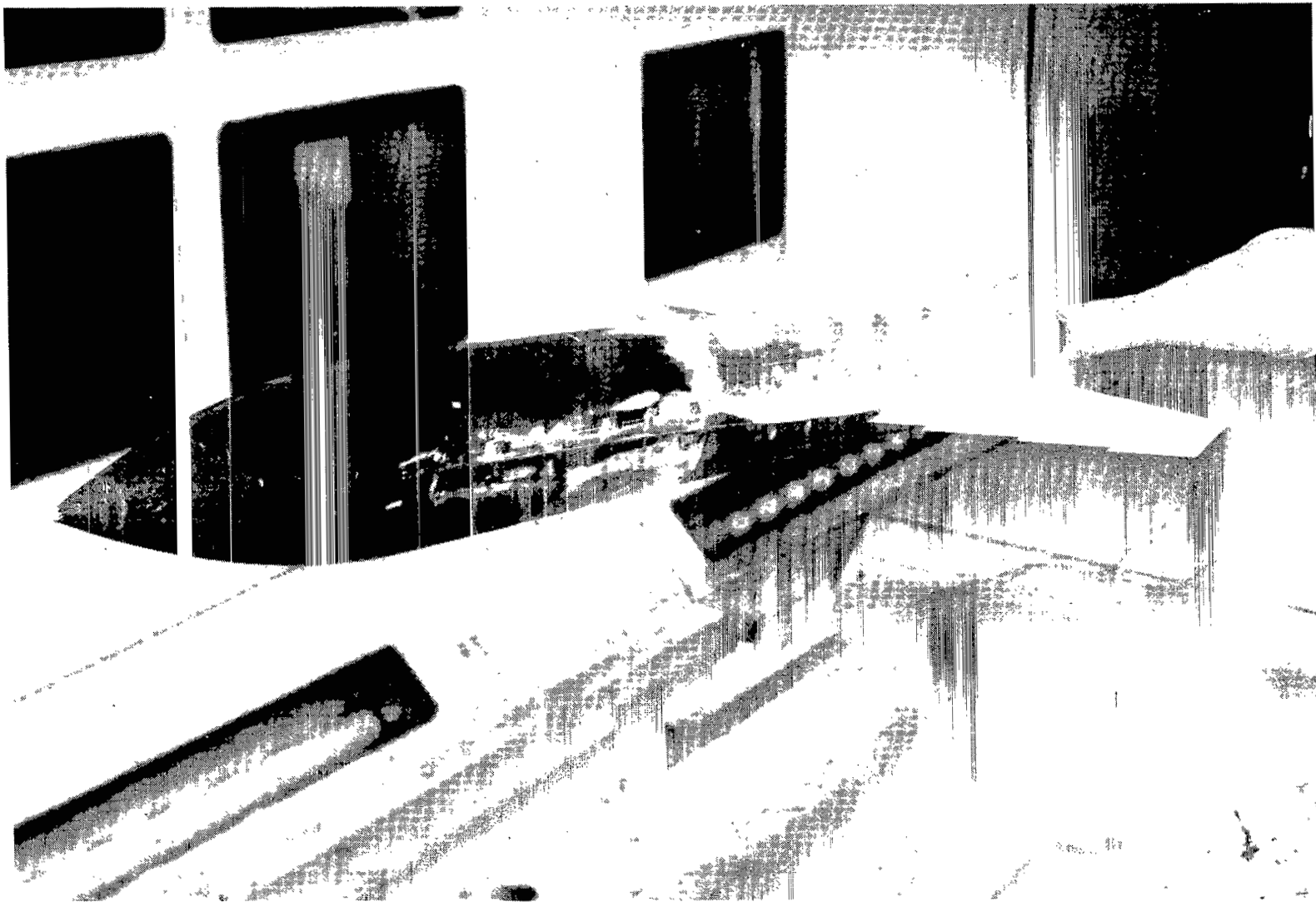
L-76-7234

(b) Flaps deflected.

Figure 3.- Concluded.
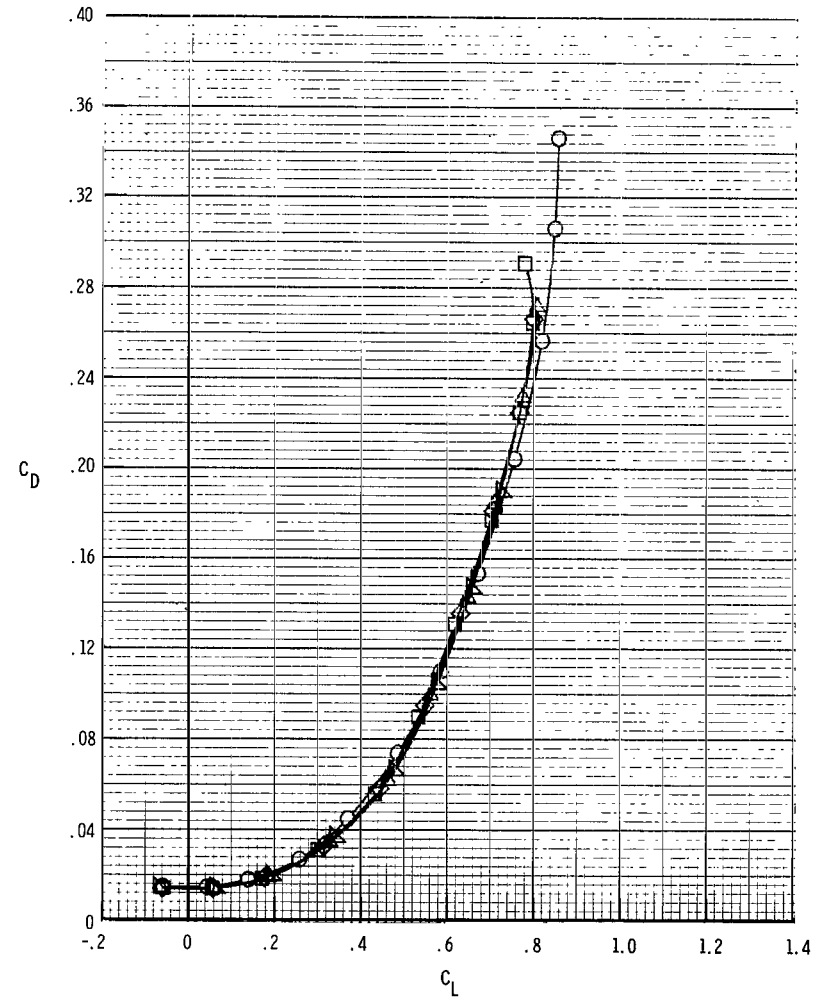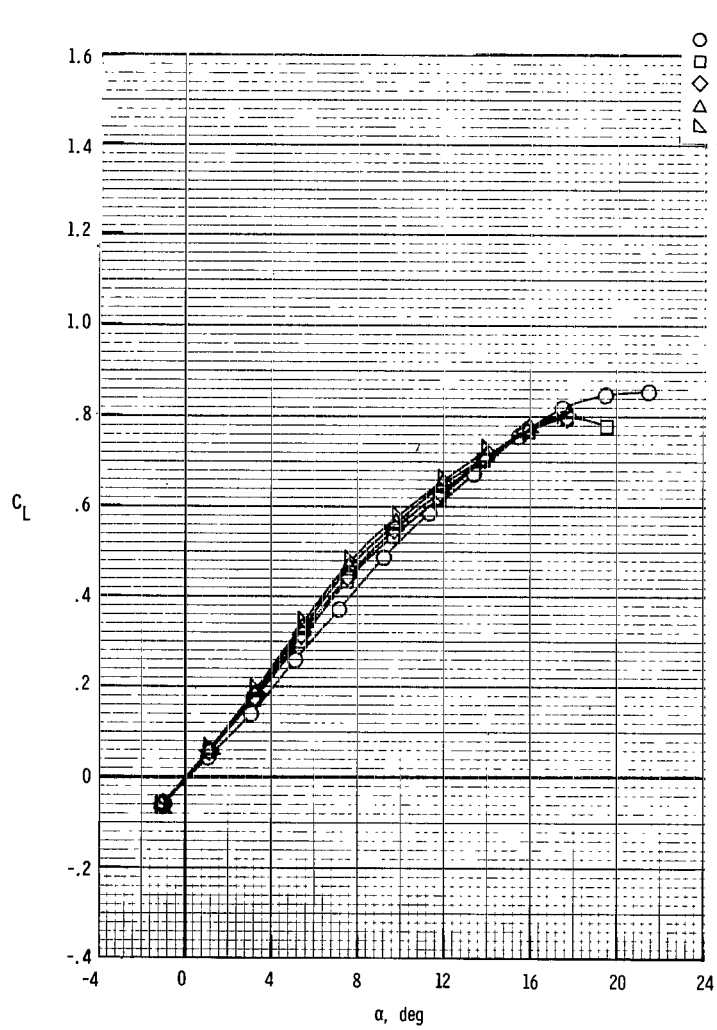
Figure 4.- Effect of Mach number on longitudinal aerodynamic characteristics for wing-fuselage configuration. $\delta_{f,1 \text{ to } 5} = 0^{\circ}$.
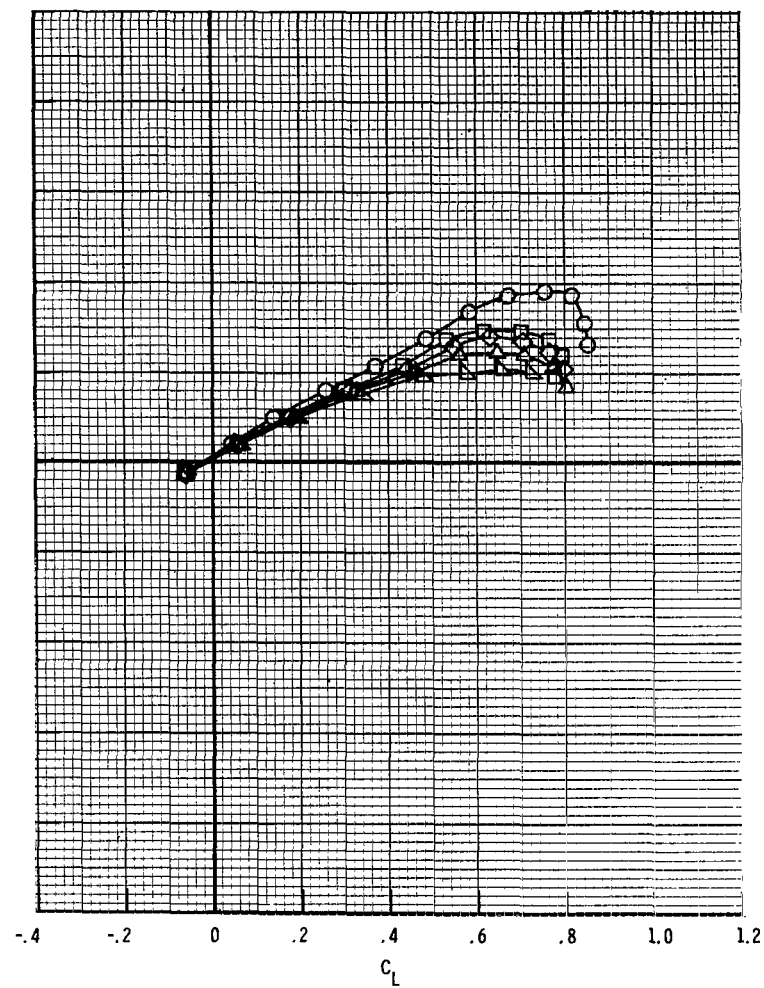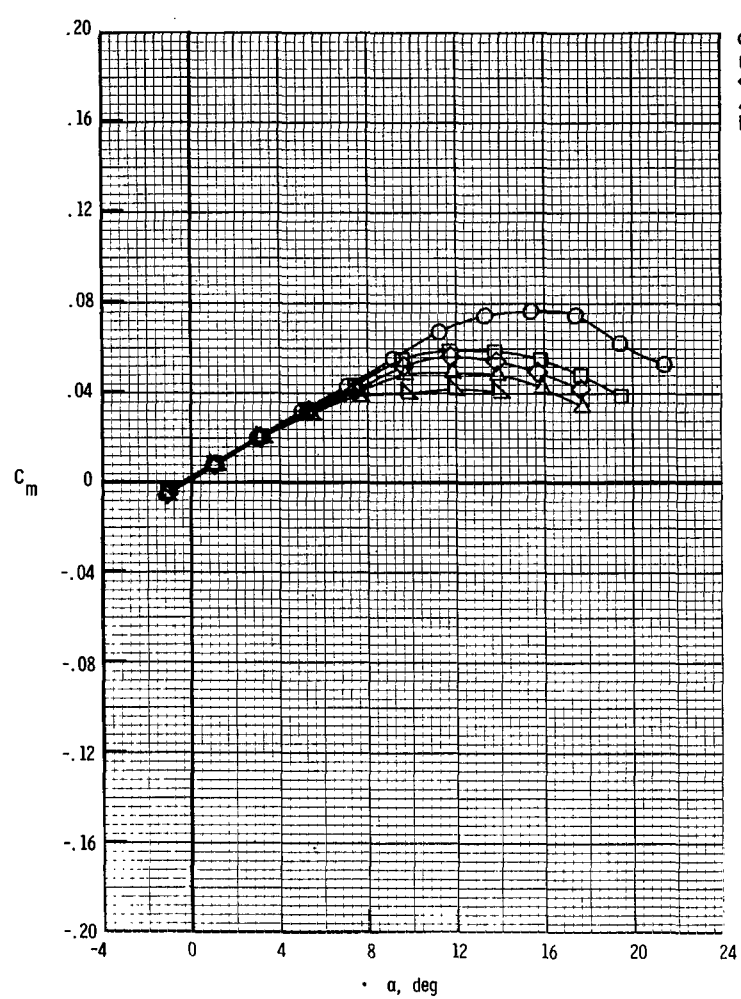
Figure 4.- Concluded.
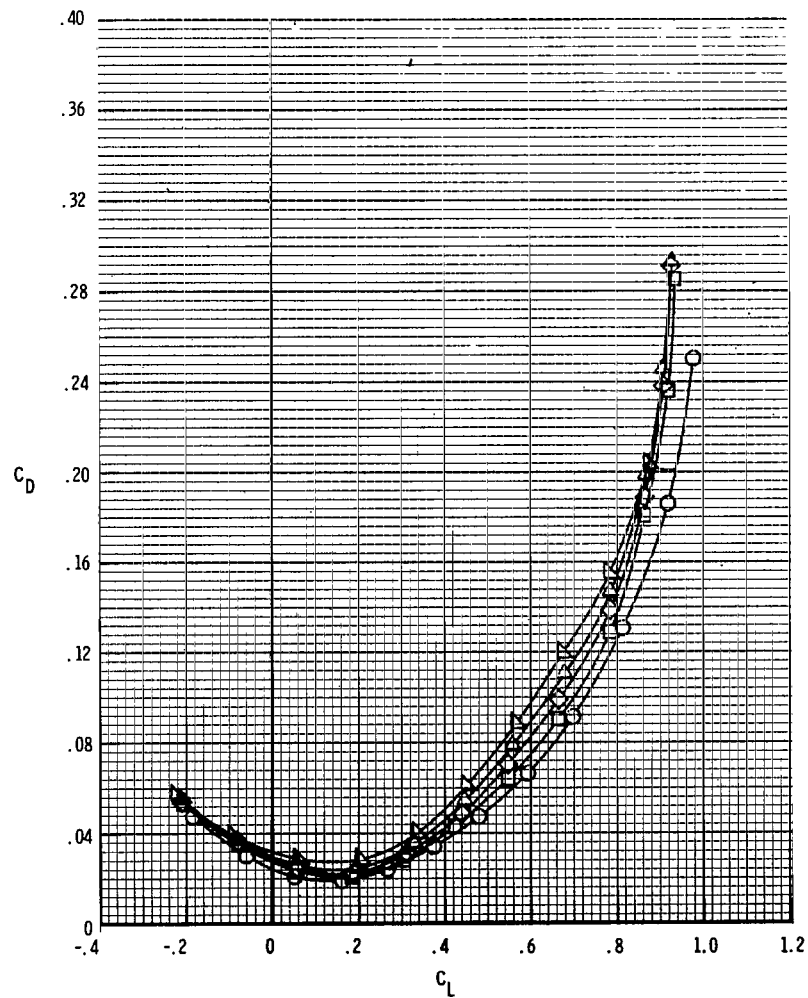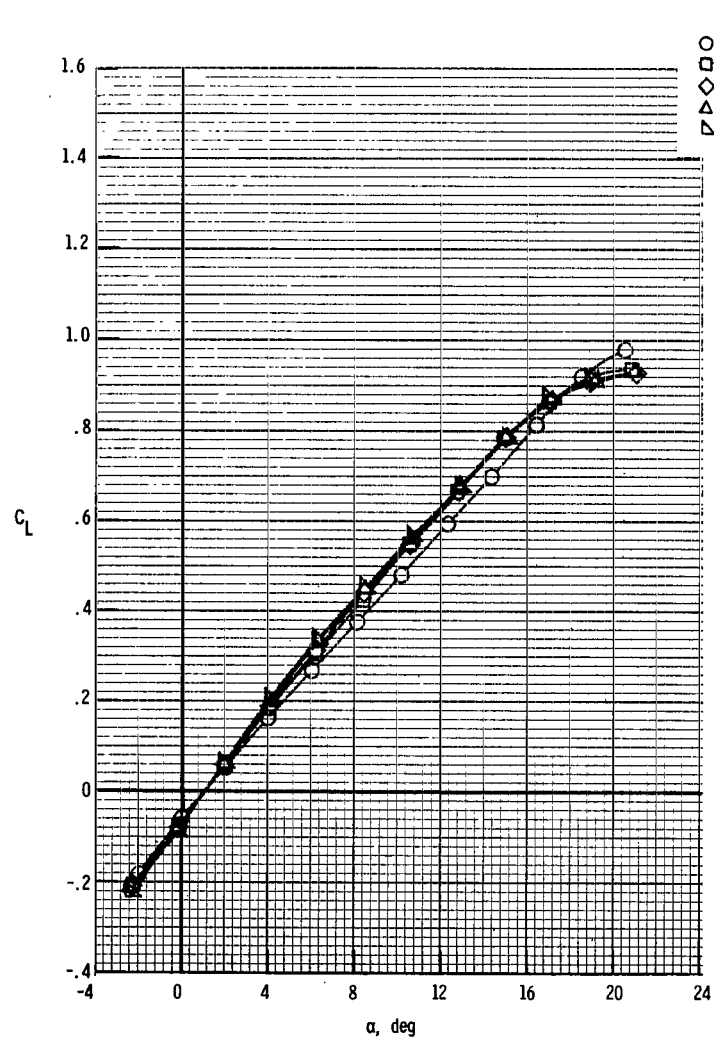
Figure 5.- Effect of Mach number on longitudinal aerodynamic characteristics for wing-fuselage configuration. $\delta_{f,1 \text{ to } 5} = -16^{\circ}$.
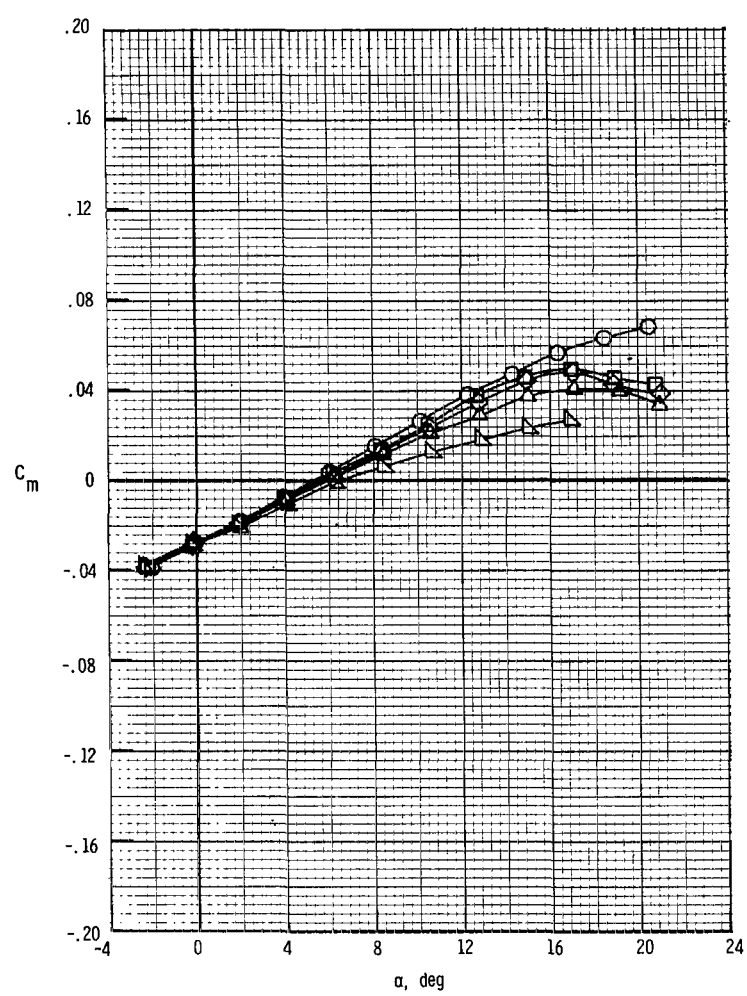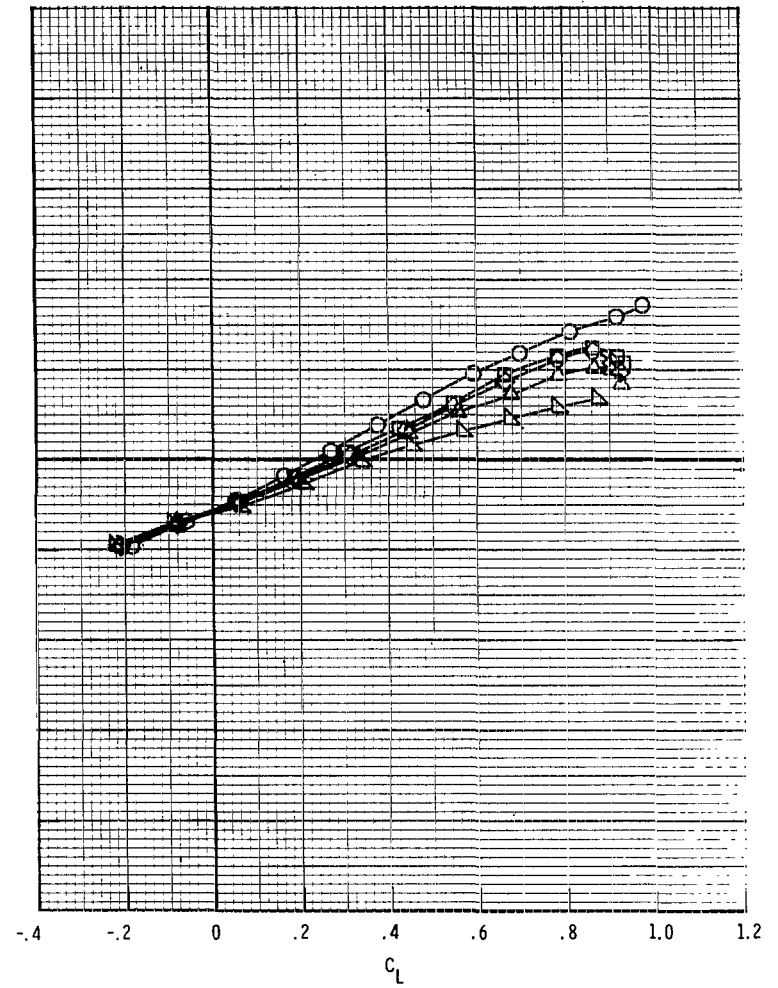
Figure 5.- Concluded.
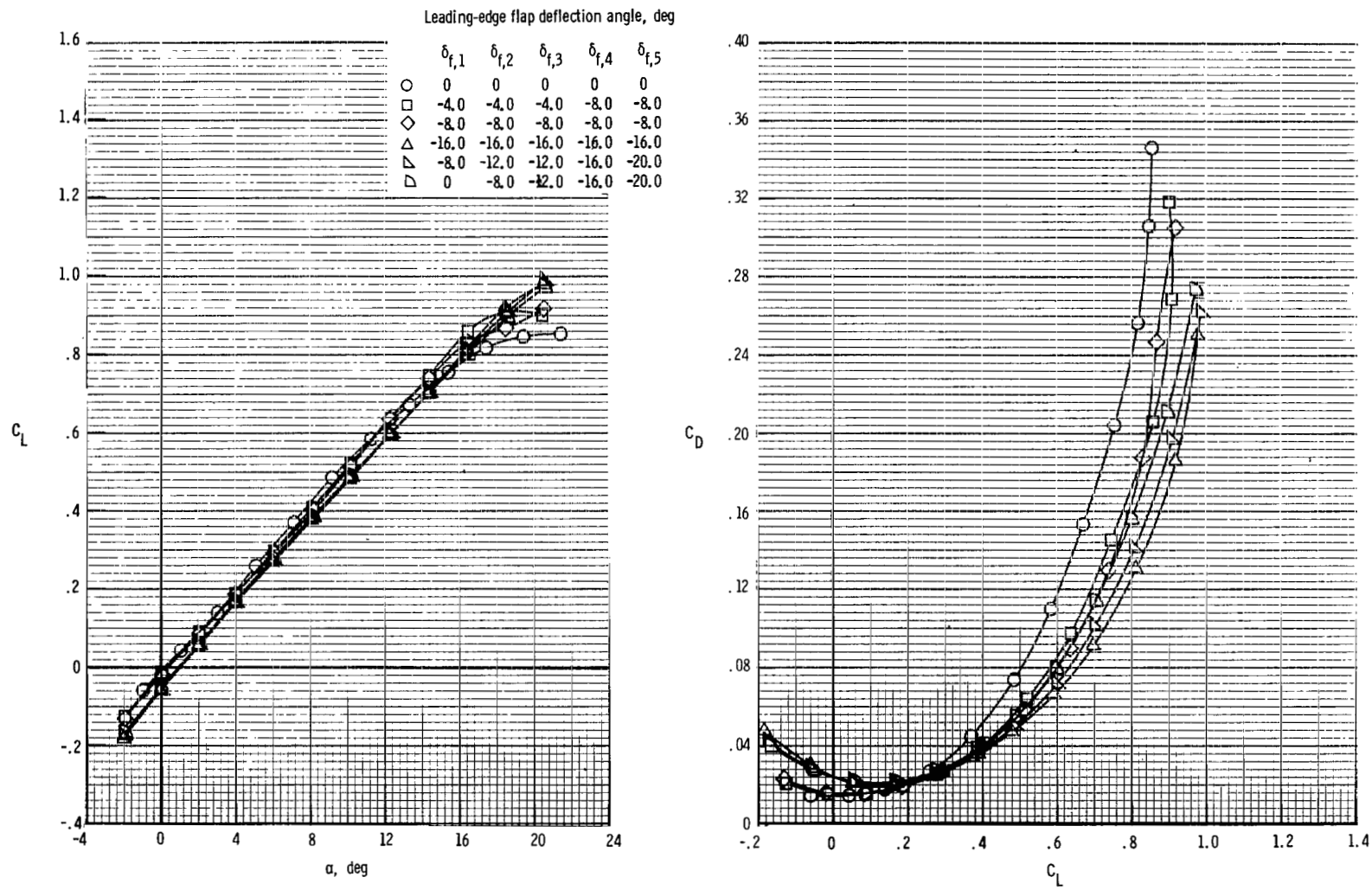
Figure 6.- Effect of wing leading-edge flap deflection on longitudinal aerodynamic characteristics for wing-fuselage configuration at M = 0.40.
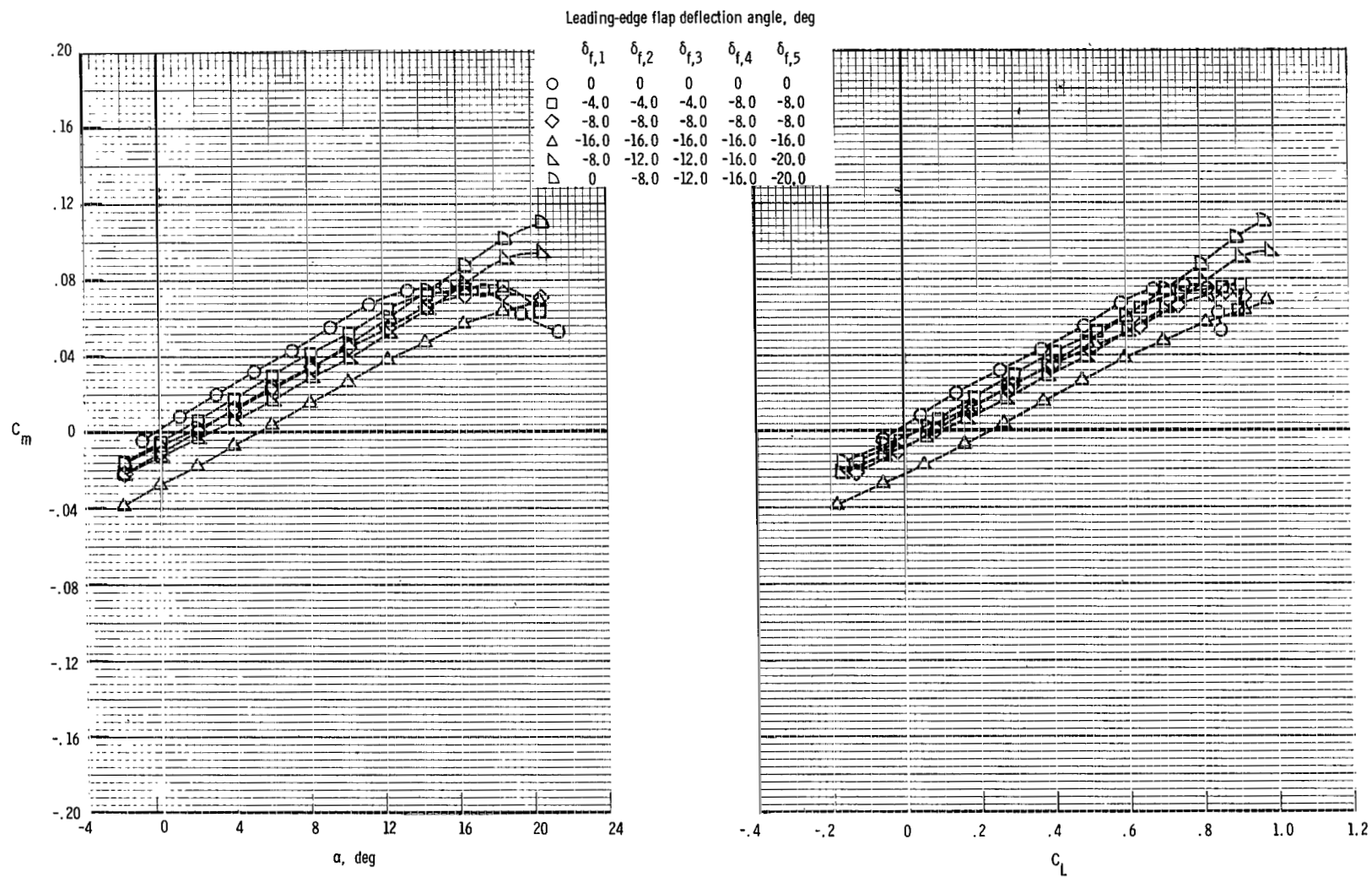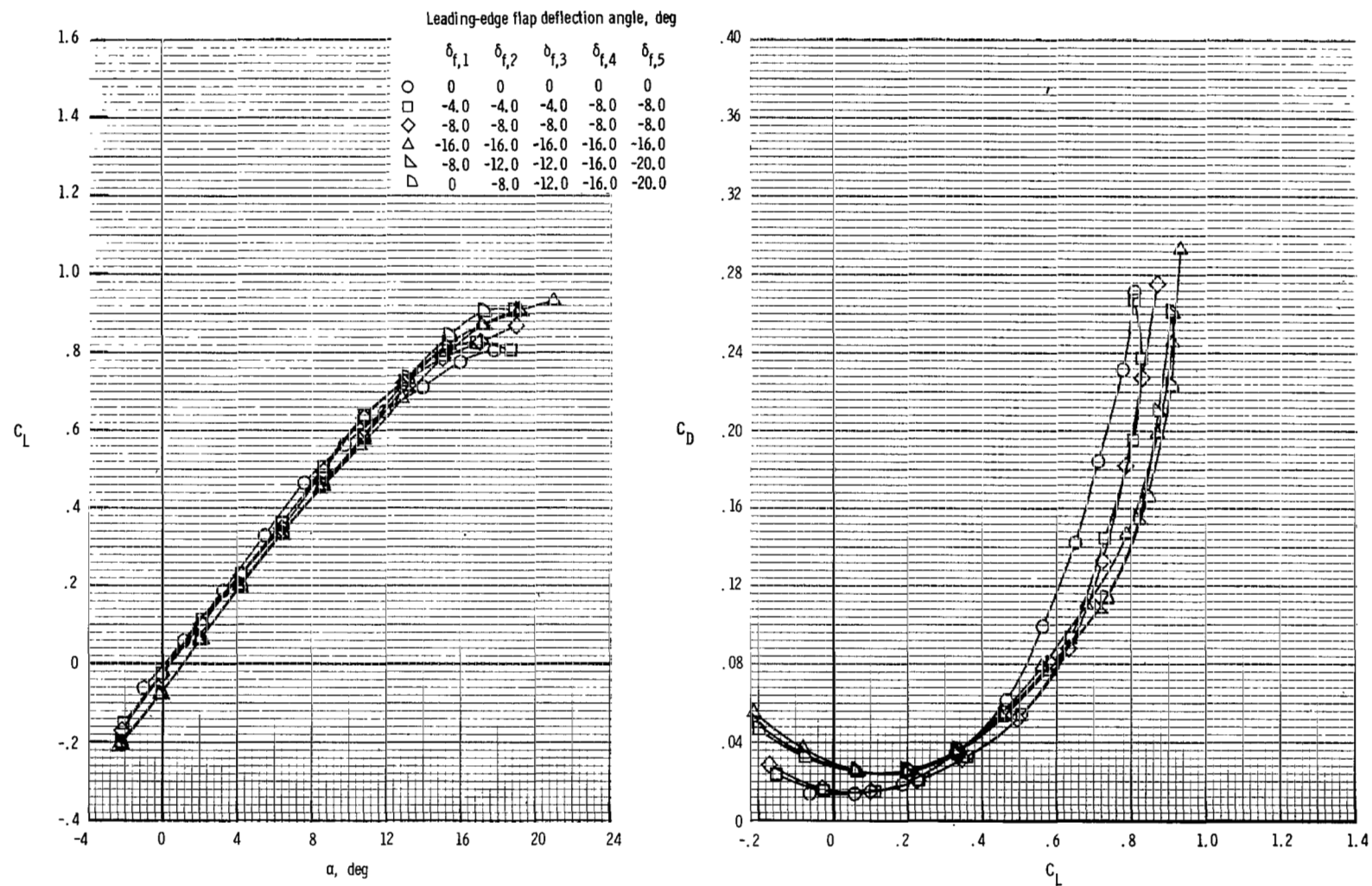
Figure 6.- Concluded.

Figure 7.- Effect of wing leading-edge flap deflection on longitudinal aerodynamic characteristics for wing-fuselage configuration at M = 0.80.
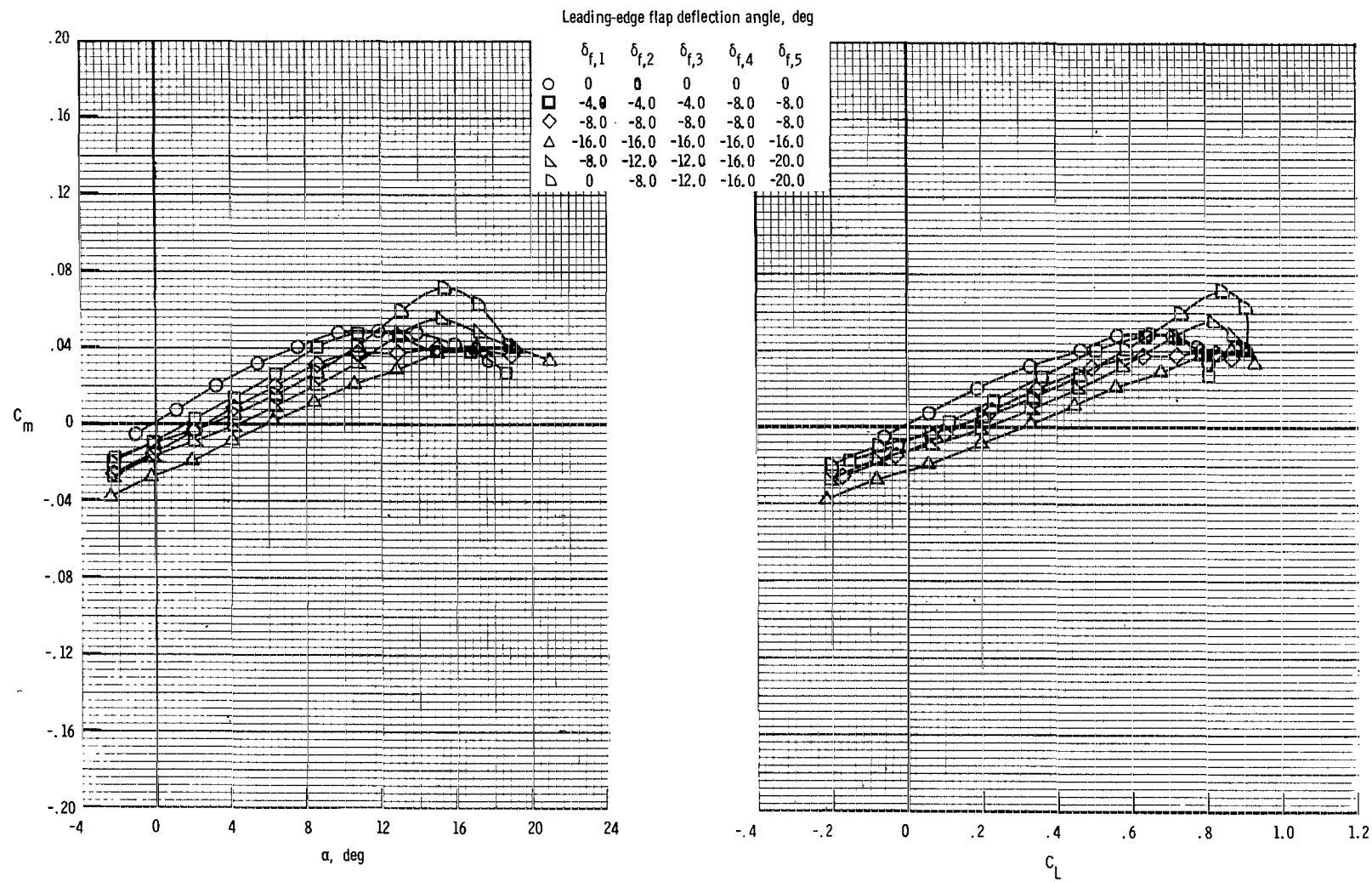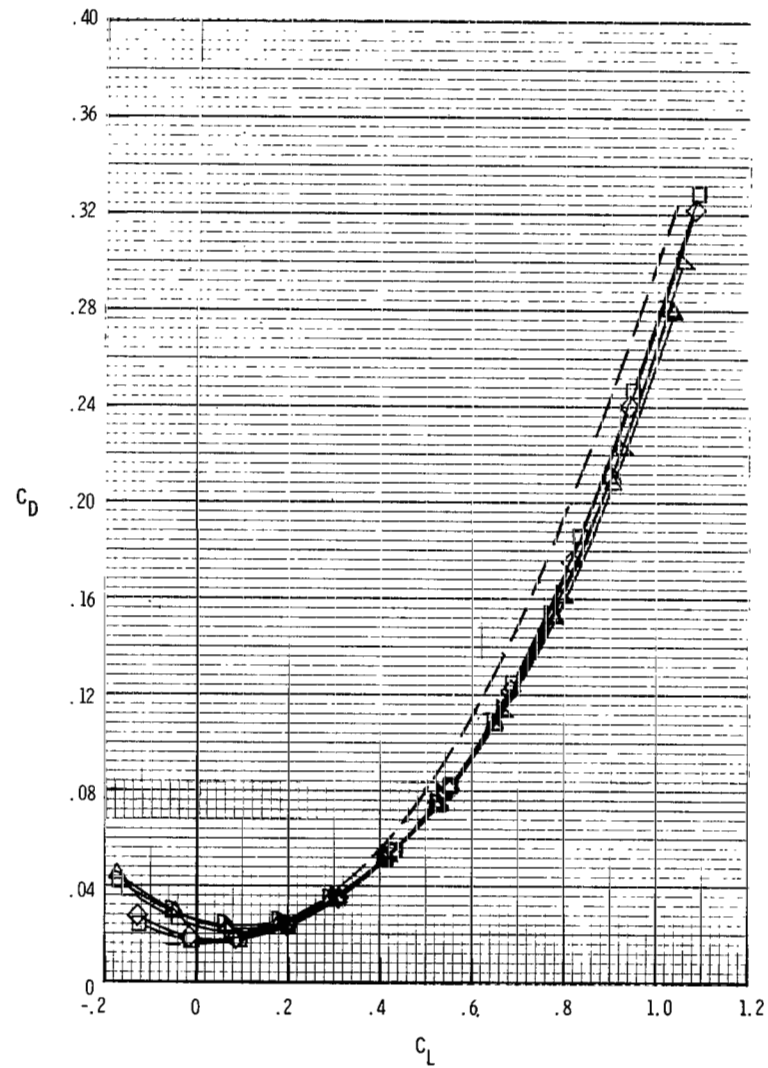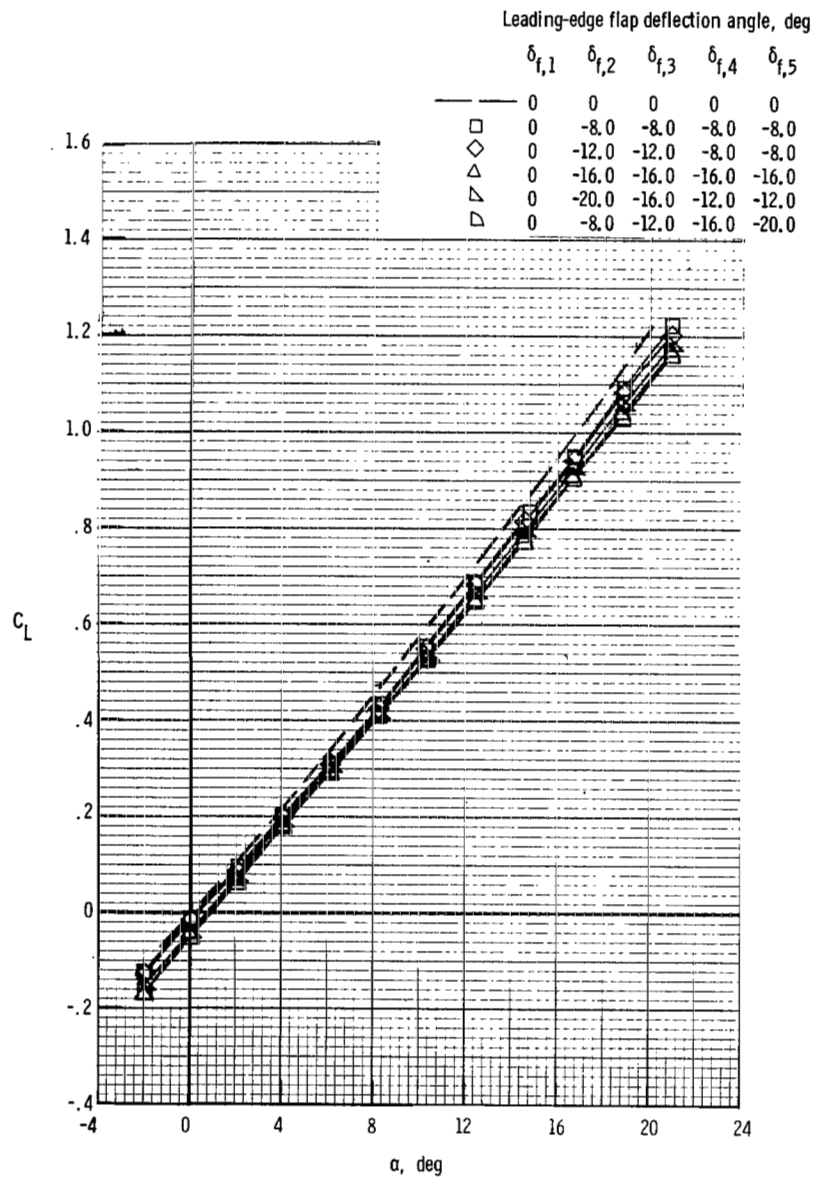
Figure 7.- Concluded.

Leading-edge flap deflection angle, deg

	$\delta_{f,1}$	$\delta_{f,2}$	$\delta_{f,3}$	$\delta_{f,4}$	$\delta_{f,5}$
——	0	0	0	0	0
□	0	-8.0	-8.0	-8.0	-8.0
◇	0	-12.0	-12.0	-8.0	-8.0
△	0	-16.0	-16.0	-16.0	-16.0
◁	0	-20.0	-16.0	-12.0	-12.0
◁	0	-8.0	-12.0	-16.0	-20.0

Figure 8.- Effect of wing leading-edge flap deflection on longitudinal aerodynamic characteristics for wing-fuselage-strake configuration at M = 0.40.
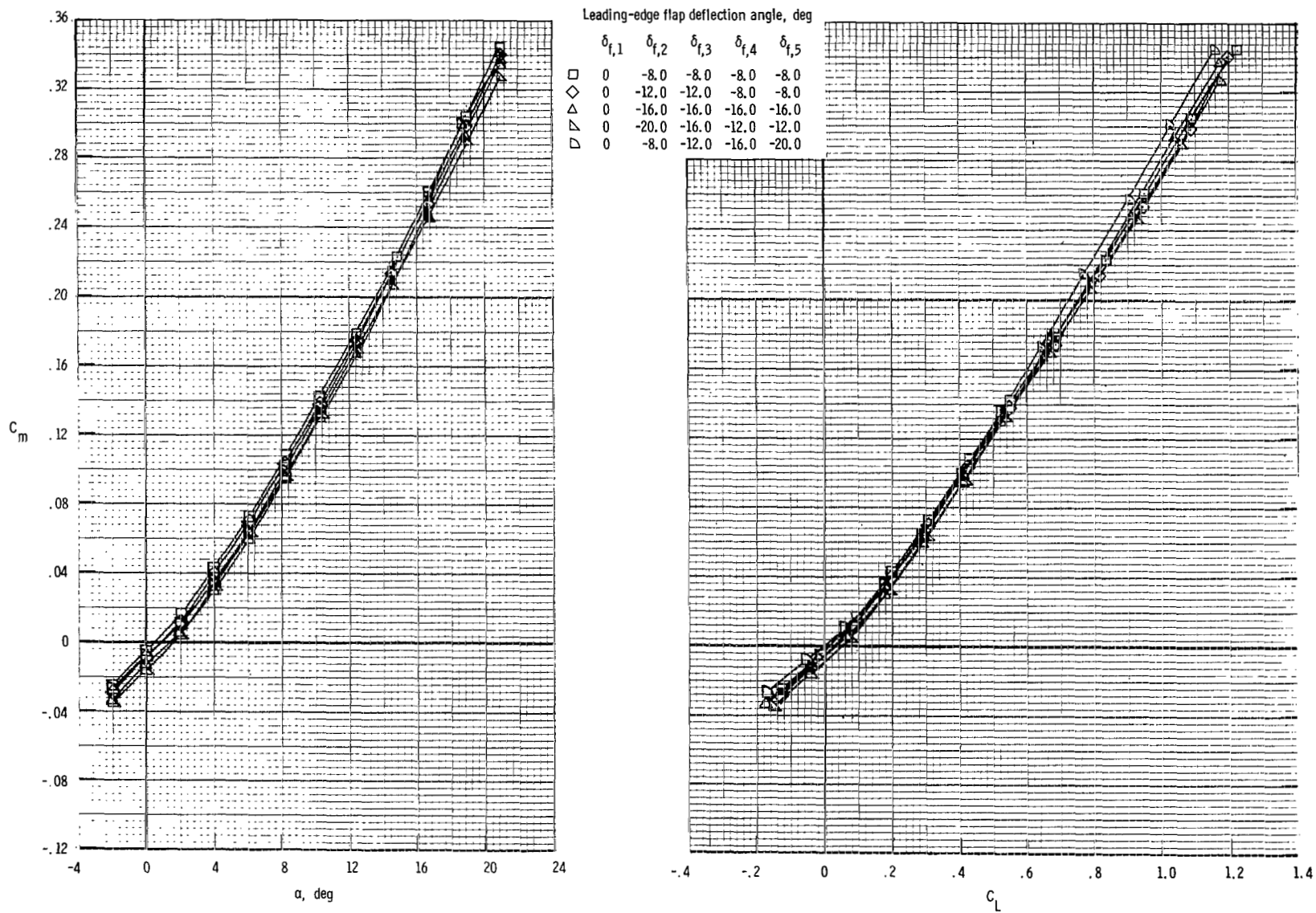
Figure 8.- Concluded.
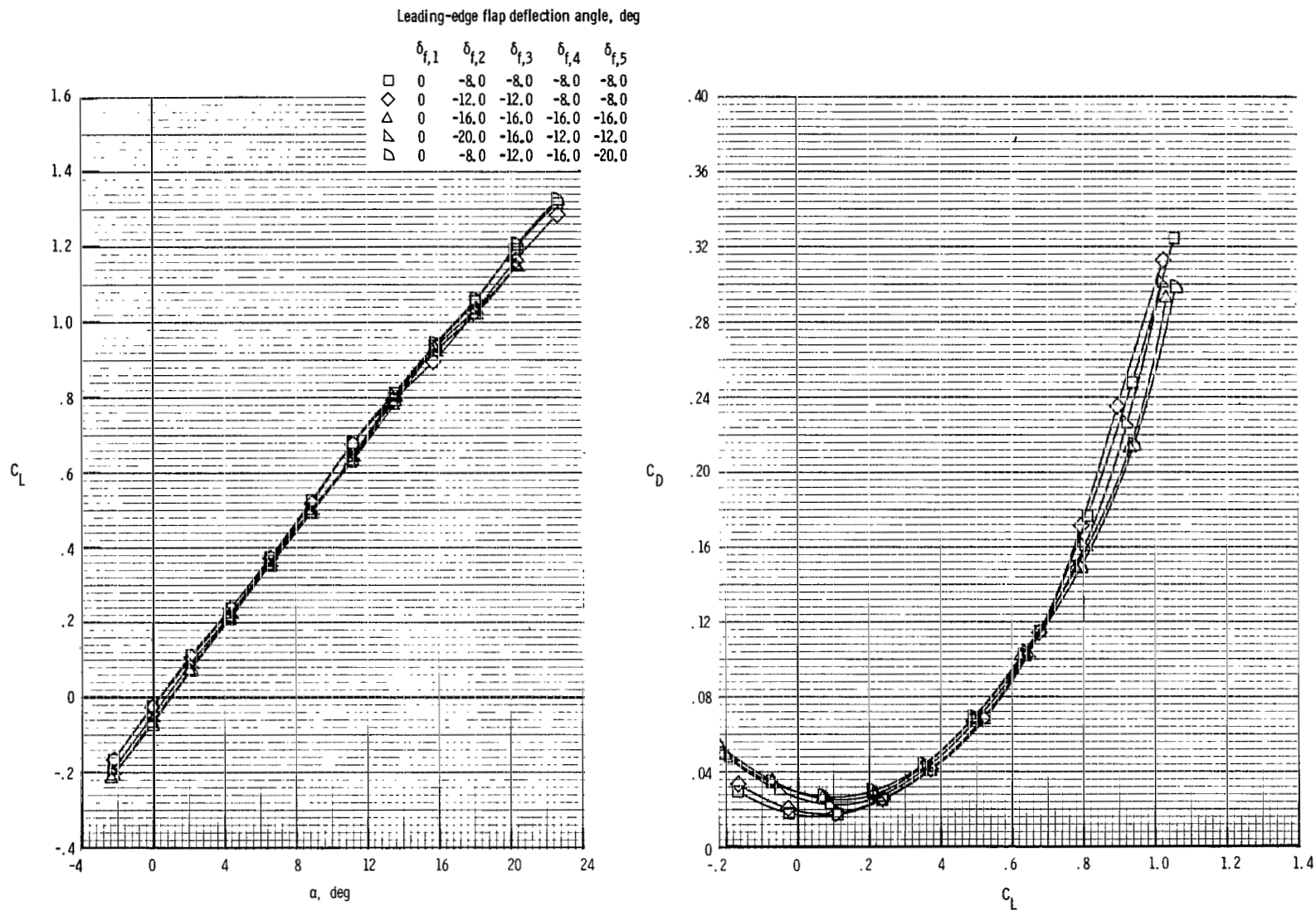
Figure 9.- Effect of wing leading-edge flap deflection on longitudinal aerodynamic characteristics for wing-fuselage-strake configuration at M = 0.80.
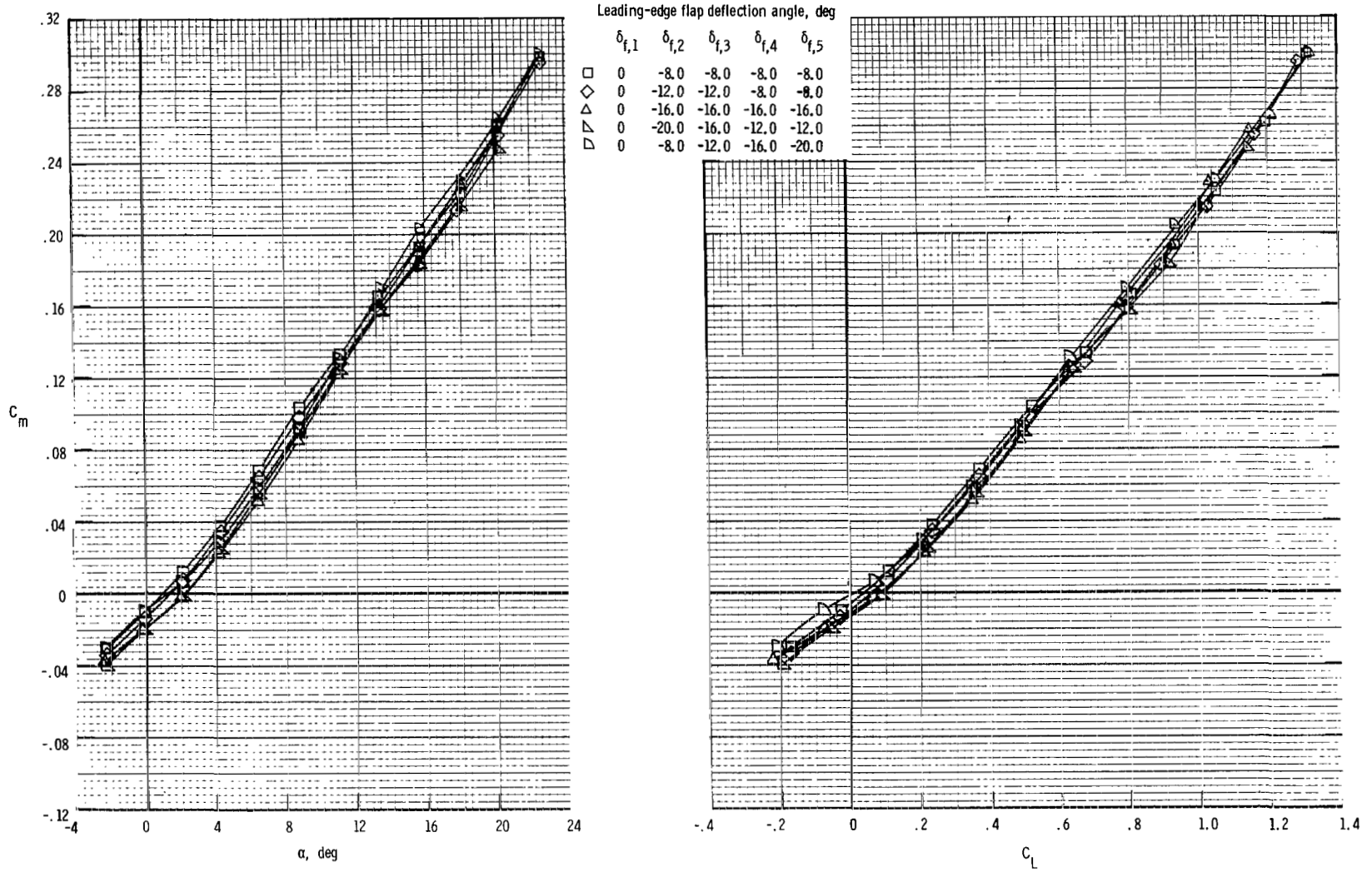
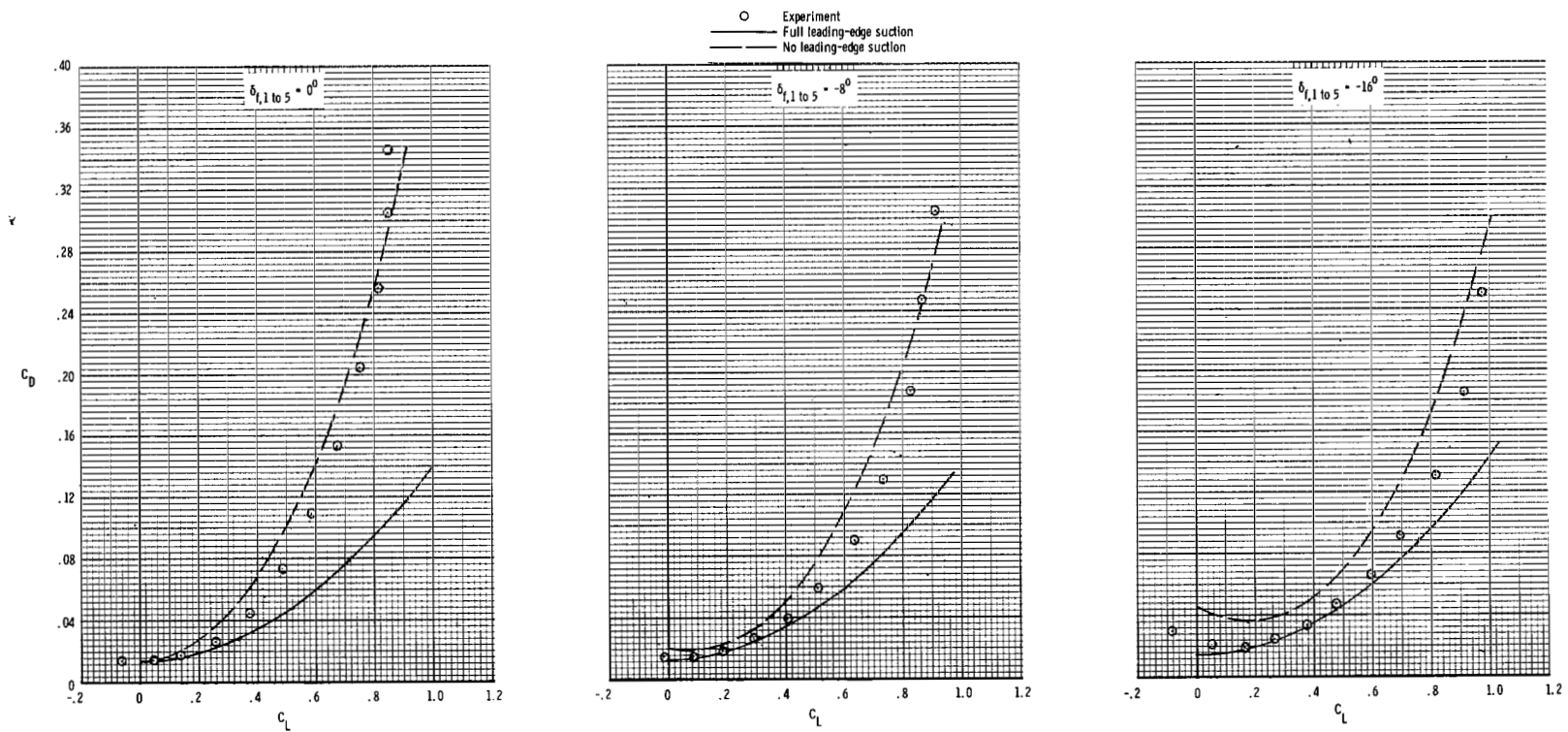|	Leading-edge flap deflection angle, deg				
	$\delta_{f,1}$	$\delta_{f,2}$	$\delta_{f,3}$	$\delta_{f,4}$	$\delta_{f,5}$
□	0	-8.0	-8.0	-8.0	-8.0
◇	0	-12.0	-12.0	-8.0	-8.0
△	0	-16.0	-16.0	-16.0	-16.0
◁	0	-20.0	-16.0	-12.0	-12.0
◁	0	-8.0	-12.0	-16.0	-20.0

Figure 9.- Concluded.

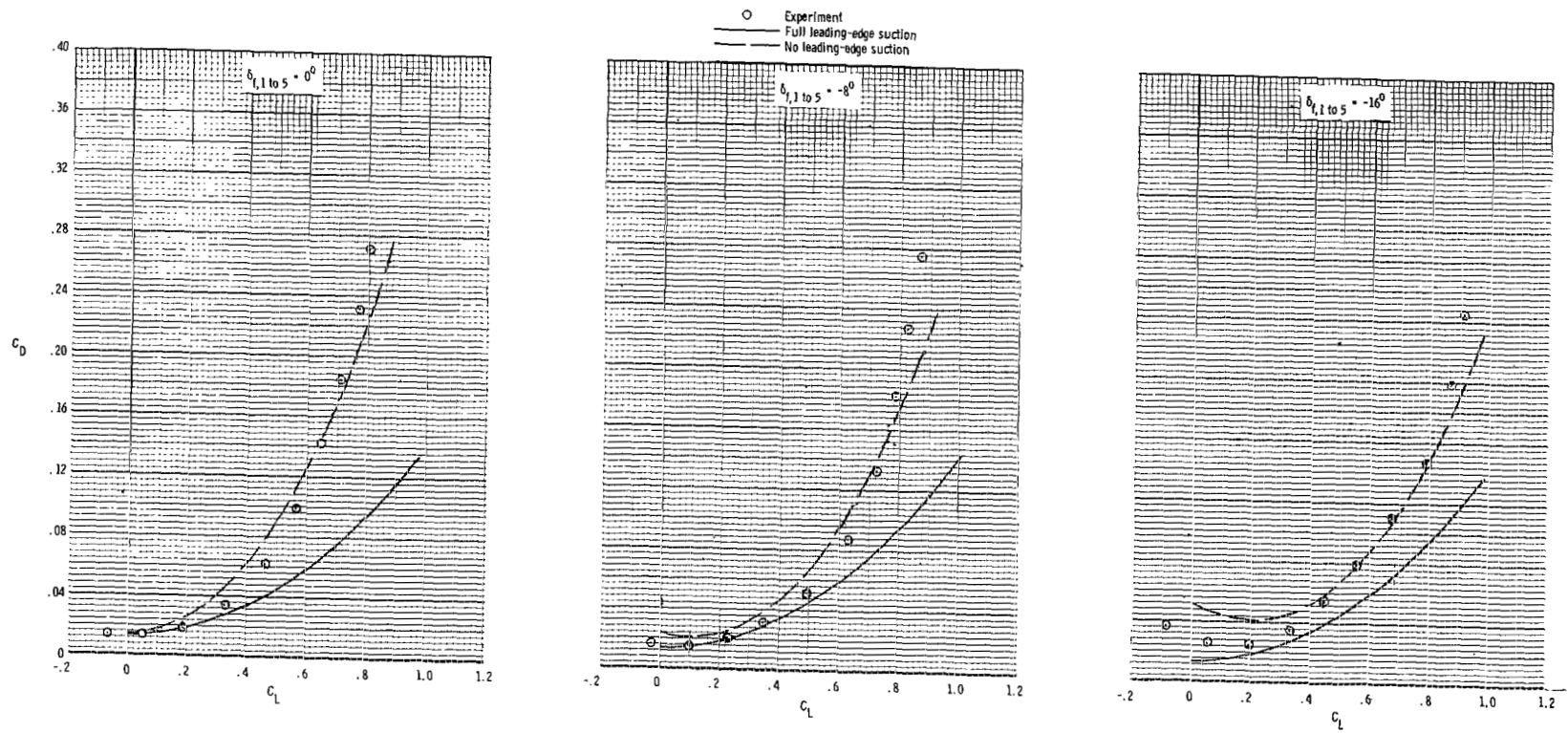Figure 10.- Comparison of theory and experiment for wing-fuselage configuration at M = 0.40.

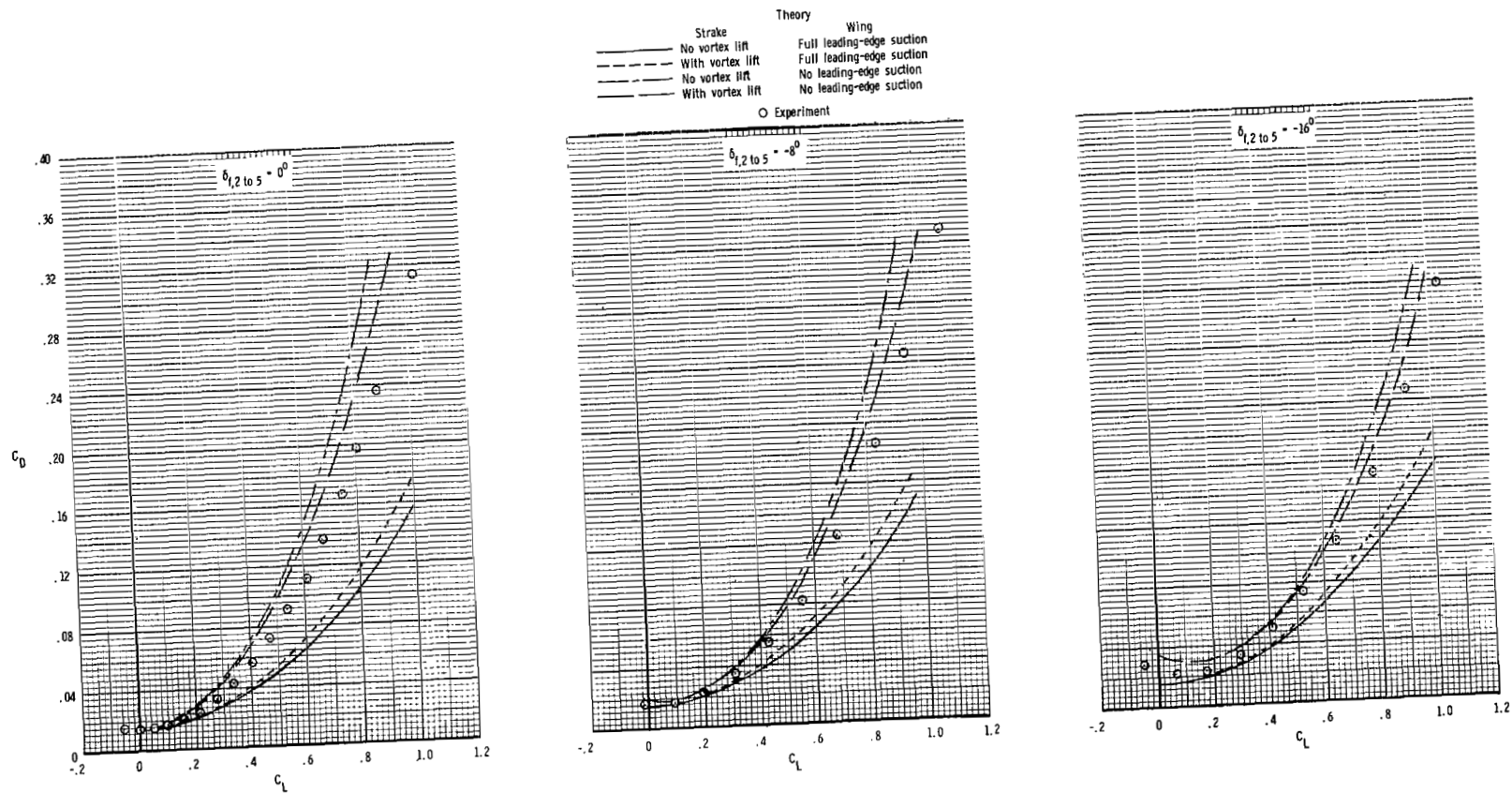Figure 11.- Comparison of theory and experiment for wing-fuselage configuration at M = 0.80.

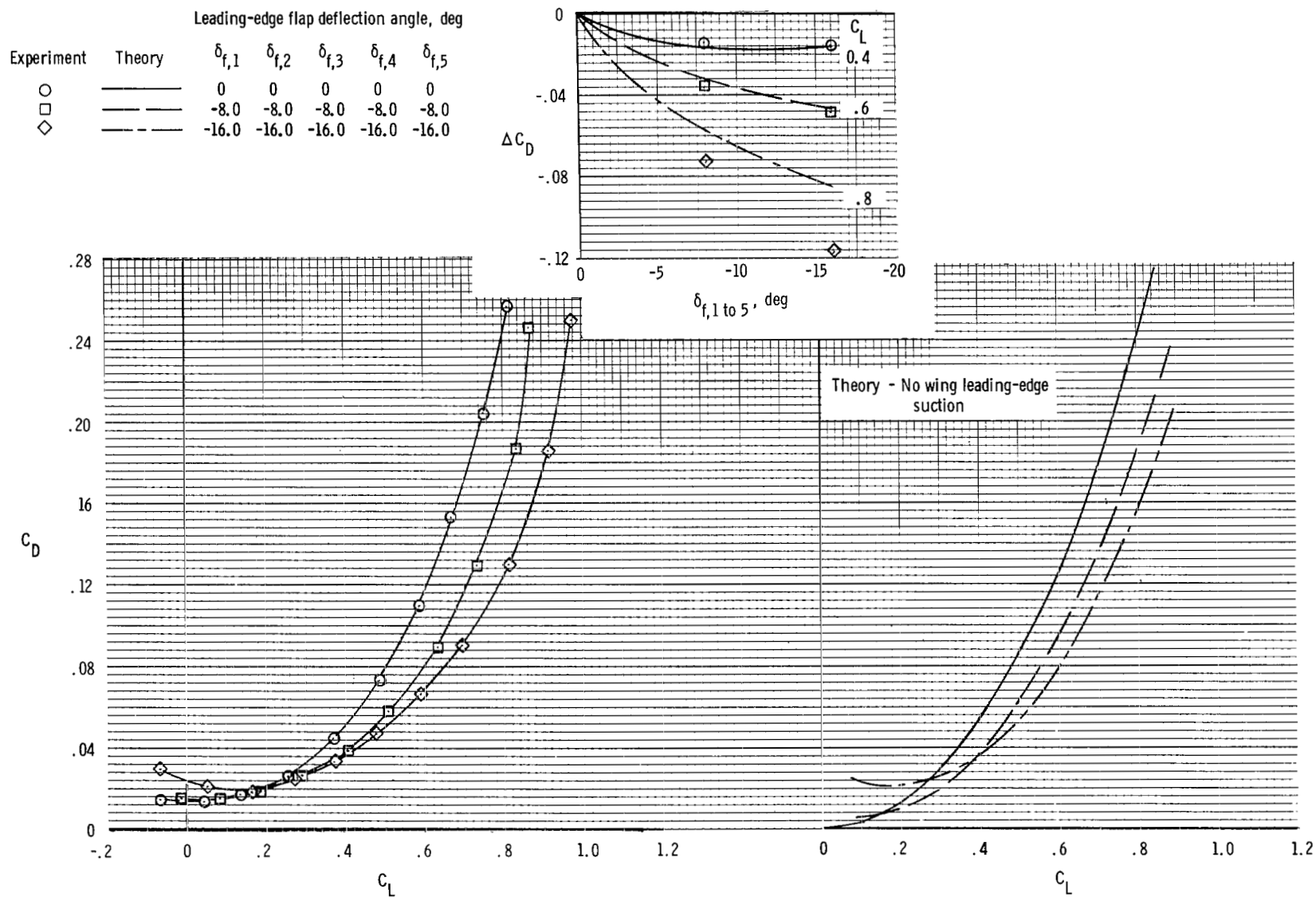Figure 12.- Comparison of theory and experiment for wing-fuselage-strake configuration at M = 0.40.

Figure 13.- Comparison of estimated and experimental increments in drag due to flap deflection for wing-fuselage configuration at M ≅ 0.40.

Leading-edge flap deflection angle, deg

Experiment	Theory	$\delta_{f,1}$	$\delta_{f,2}$	$\delta_{f,3}$	$\delta_{f,4}$	$\delta_{f,5}$
○	——	0	0	0	0	0
□	— —	-8.0	-8.0	-8.0	-8.0	-8.0
◇	— ·· —	-16.0	-16.0	-16.0	-16.0	-16.0

C_L

0.4

.6

.8

ΔC_D

$\delta_{f,1 \text{ to } 5}$, deg

C_D
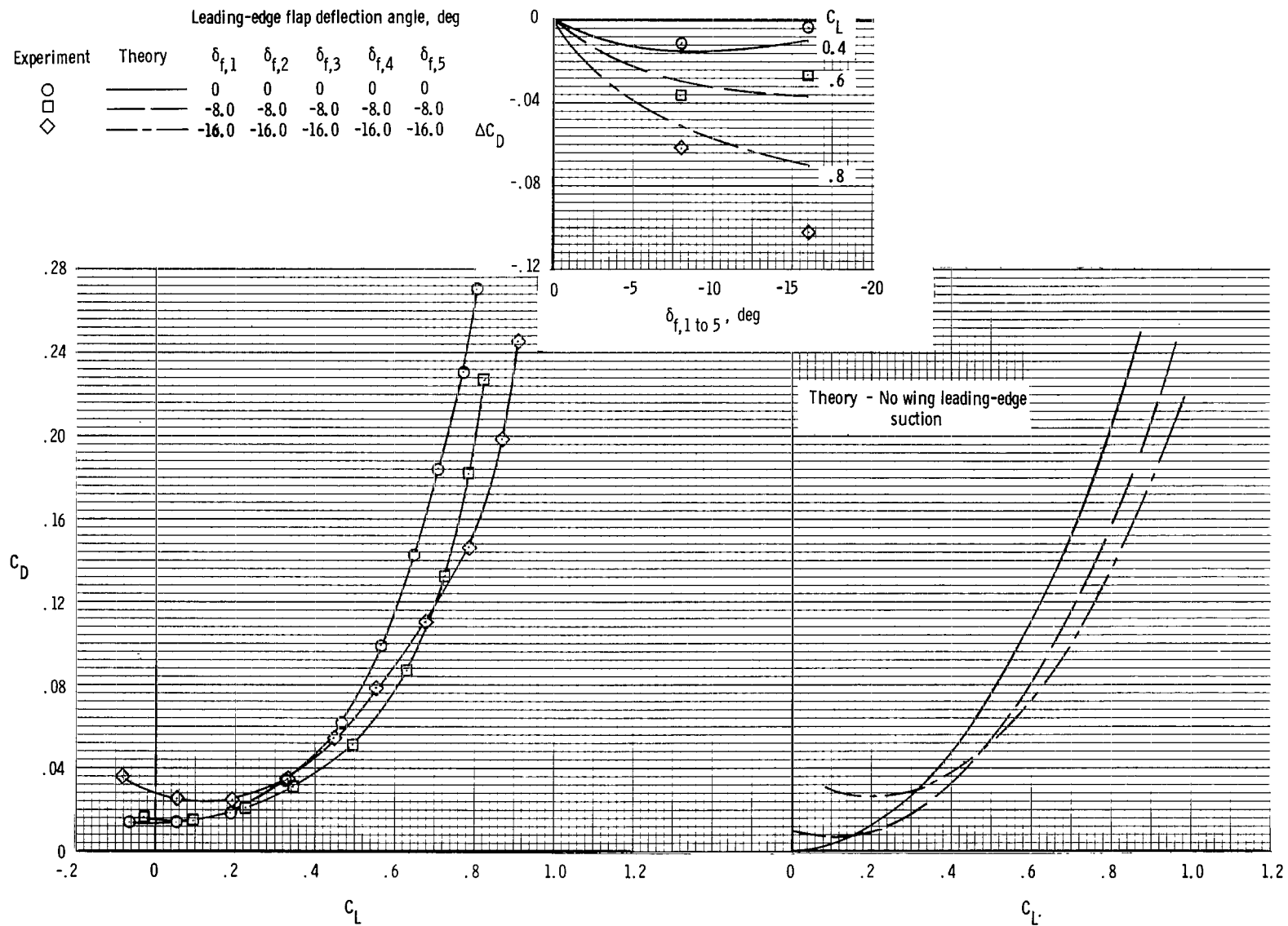
Theory – No wing leading-edge suction

C_L

$C_{L'}$

Figure 14.- Comparison of estimated and experimental increments in drag due to flap deflection for wing-fuselage configuration at M = 0.80.
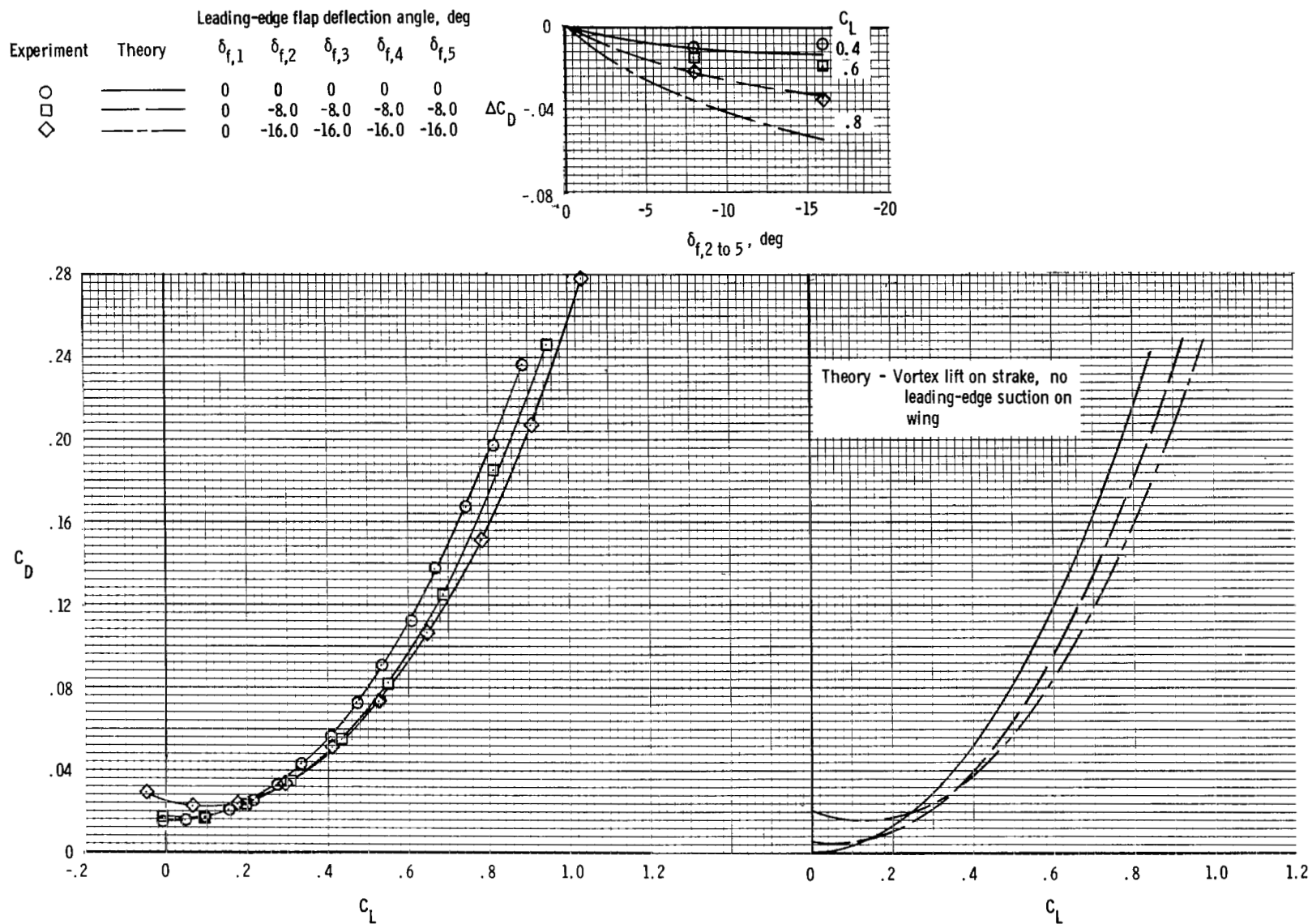
Figure 15.- Comparison of estimated and experimental increments in drag due to flap deflection for wing-fuselage-strake configuration at M = 0.40.
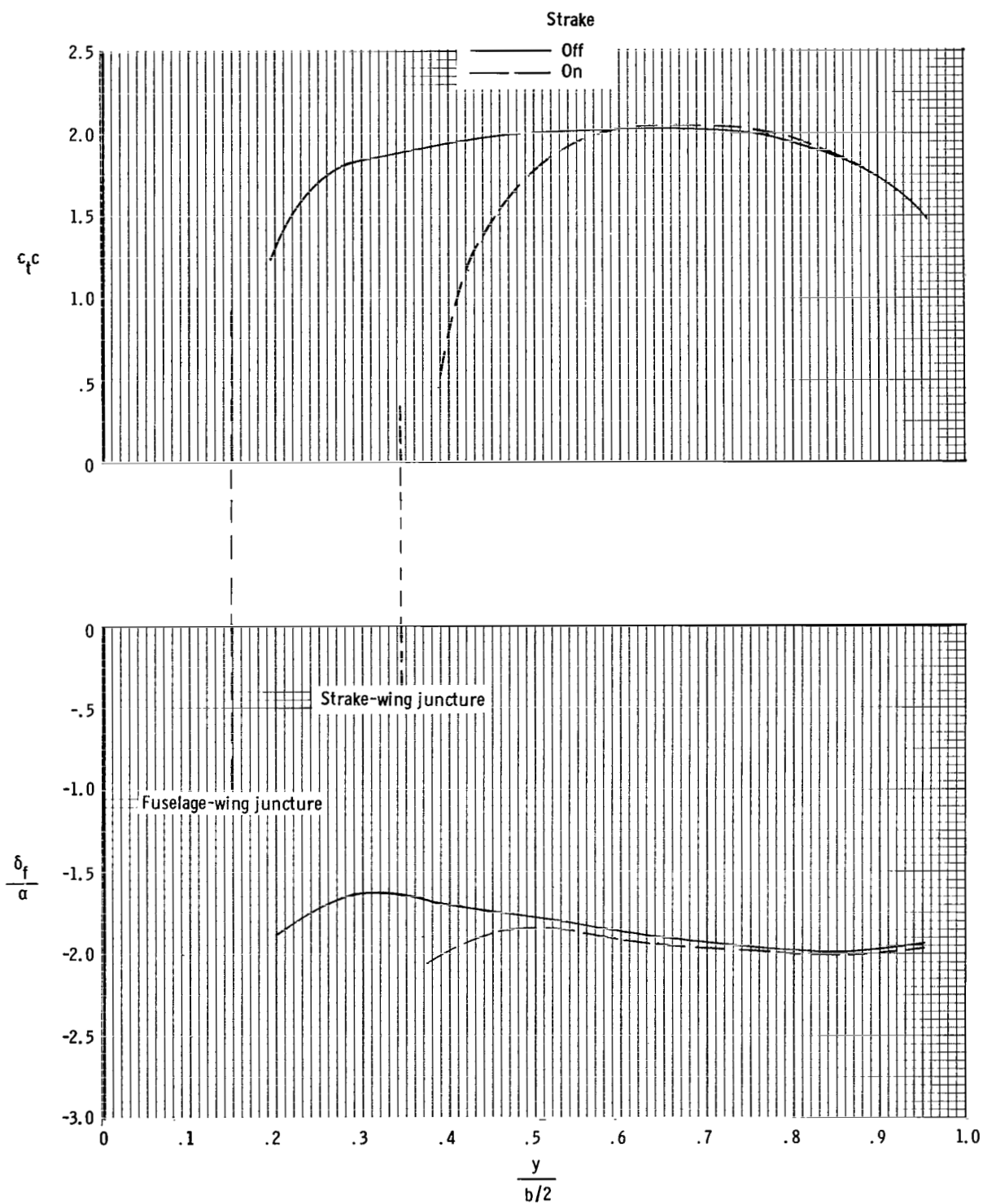
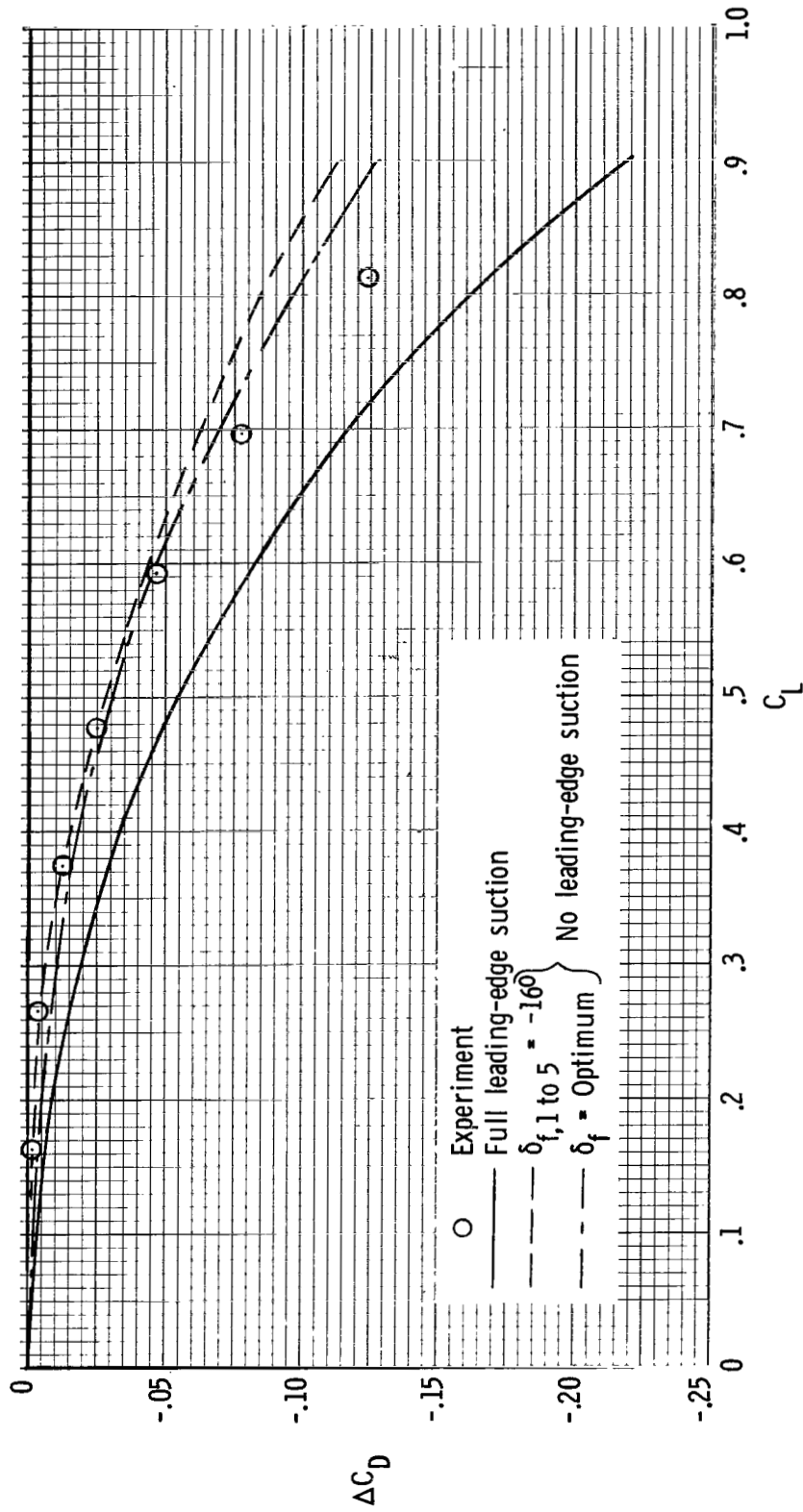Figure 16.- Variation of optimum flap-deflection angle and wing leading-edge thrust across wing span at M = 0.40.

Figure 17.– Variation of drag due to flap deflection compared with estimate for wing-fuselage configuration at M = 0.40.
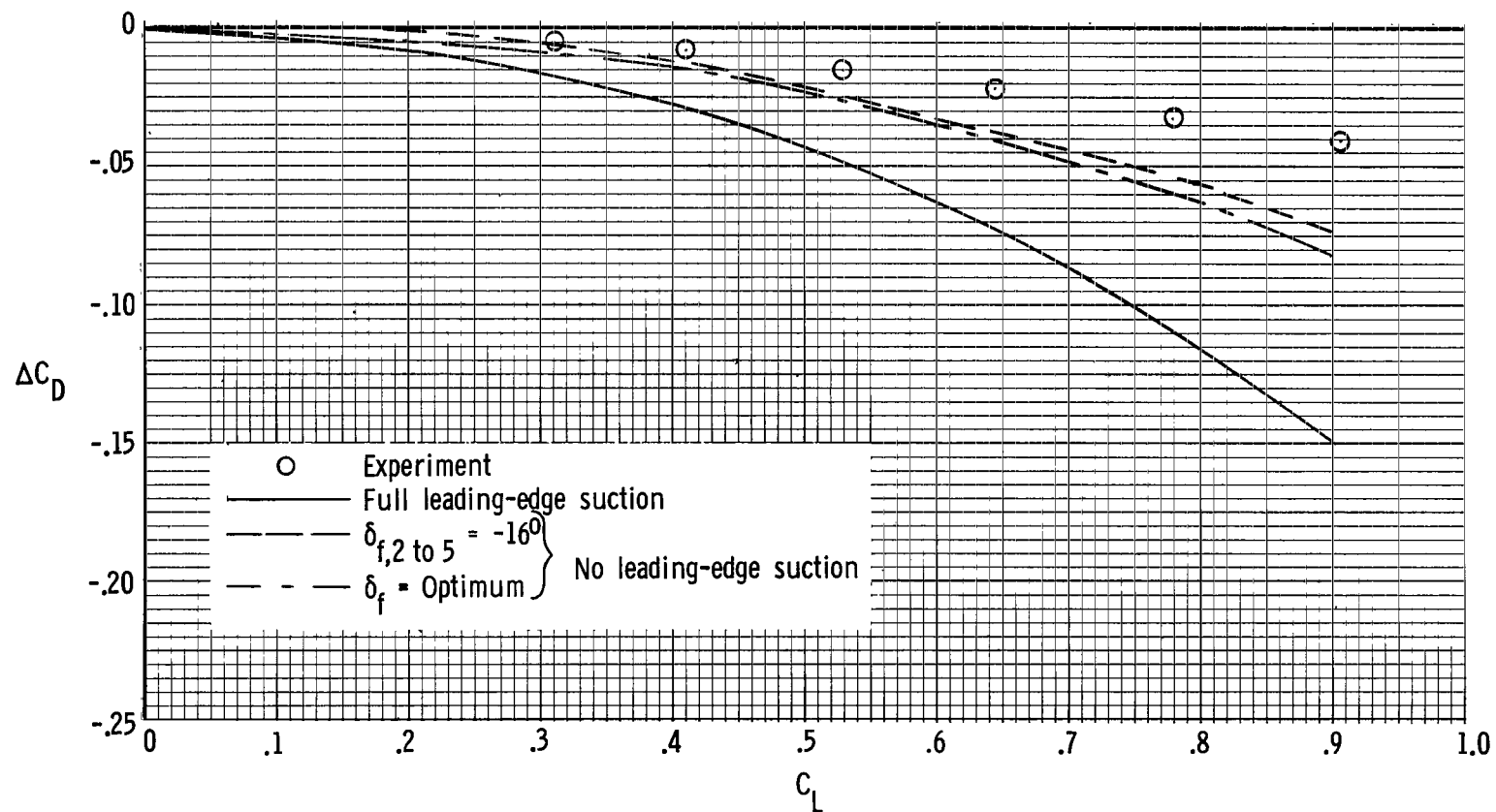
Figure 18.- Variation of drag due to flap deflection compared with estimate for wing-fuselage-strake configuration at M = 0.40.

1. Report No. NASA TP-1351	2. Government Accession No.	3. Recipient's Catalog No.
4. Title and Subtitle EFFECTS OF WING LEADING-EDGE FLAP DEFLECTIONS ON SUBSONIC LONGITUDINAL AERODYNAMIC CHARACTERISTICS OF A WING-FUSELAGE CONFIGURATION WITH A 44° SWEPT WING		5. Report Date November 1978
		6. Performing Organization Code
7. Author(s) William P. Henderson		8. Performing Organization Report No. L-12481
		10. Work Unit No. 505-11-23-00
9. Performing Organization Name and Address NASA Langley Research Center Hampton, VA 23665		11. Contract or Grant No.
		13. Type of Report and Period Covered Technical Paper
12. Sponsoring Agency Name and Address National Aeronautics and Space Administration Washington, DC 20546		
		14. Sponsoring Agency Code

15. Supplementary Notes

16. Abstract

An investigation has been conducted to determine the effects of wing leading-edge flap deflections on the subsonic longitudinal aerodynamic characteristics of a wing-fuselage configuration with a 44° swept wing. The tests were conducted at Mach numbers from 0.40 to 0.85, corresponding to Reynolds numbers (based on wing mean geometric chord) of 2.37×10^6 to 4.59×10^6 and at angles of attack from -3° to 22°. The configurations under study included a wing-fuselage configuration and a wing-fuselage-strake configuration. Each configuration had multisegmented, constant-chord leading-edge flaps which could be deflected independently or in various combinations.

17. Key Words (Suggested by Author(s)) Aerodynamics Leading-edge flap performance Stability Vortex lift	18. Distribution Statement Unclassified – Unlimited Subject Category 02

19. Security Classif. (of this report) Unclassified	20. Security Classif. (of this page) Unclassified	21. No. of Pages 35	22. Price* $4.50

National Aeronautics and
Space Administration

Washington, D.C.
20546

THIRD-CLASS BULK RATE

Postage and Fees Paid
National Aeronautics and
Space Administration
NASA-451

U.S.MAIL

```
   5    1 1U,A,        092278 S00903DS
DEPT OF THE AIR FORCE
AF WEAPONS LABORATORY
ATTN: TECHNICAL LIBRARY (SUL)
KIRTLAND AFB NM 87117
```

NASA

POSTMASTER: If Undeliverable (Section 158
Postal Manual) Do Not Return